Chinese Chemical Letters 35 (2024) 109472

Contents lists available at ScienceDirect

Chinese Chemical Letters

journal homepage: www.elsevier.com/locate/cclet

Porous carbon catalysis in sustainable synthesis of functional heterocycles: An overview

Uttam Pandurang Patil

Department of Chemistry, ACS College, Shivaji University, Palus 416310, MS, India

ARTICLE INFO

Article history:
Received 23 September 2023
Revised 19 December 2023
Accepted 28 December 2023
Available online 1 January 2024

Keywords:
Sustainable chemistry
Heterogeneous catalysts
Porous carbons
Heterocycles synthesis

ABSTRACT

Heterogeneous porous carbon (PC) materials have gained unique importance in the catalysis community due to their captivating properties, including high specific surface area, tunable porosity, and functionality. PC can play a prominent role in the sustainable synthesis of functional heterocycles, as they are a low-cost alternative while being an efficient and user-friendly material. This review examines the preparation and applicability of these carbonaceous materials used as catalysts or support for biologically active heterocycles synthesis, including hydrogenation, oxidation, oxidative dehydrogenation, cross-coupling, and other organic reactions. Moreover, the challenges, potential future development directions, and opportunities in the synthesis of potent bioactive heterocycles over PC materials have been addressed. This review will inspire further research to explore novel PC materials and their implications in heterocyclization.

1. Introduction

Catalysts are the jewel in the crown of the chemical industry, accelerating reaction kinetics and augmenting the efficiency of desired reaction pathways [1]. Since the term "catalysis" was introduced as early as 1835 by Johns Jakob Berzelius, catalysis has grown in vital importance to the world economy [2]. It has been estimated that most chemical processes require 80% of heterogeneous catalysts, 15% of homogeneous catalysts, and about 5% of biocatalysts [3]. In recent inclination, heterogeneous catalysts have gained unprecedented importance because of their versatile properties with faster, large-scale production and selective product formation. Among a diverse range of heterogeneous catalysts, porous carbons (PCs) have been immensely appealing as one of the most significant and proactive catalysts since the last decade due to their large specific surface area, hierarchical porosity, unique morphologies, high thermal, chemical, and mechanical stabilities, excellent electron conductivity, and tunable pore structures. With these versatile properties, they are also cost-effective, and environmentally friendly catalytic materials [4]. They also find significant applications in various fields, such as adsorption, separation, medicine, and energy storage and conversion [5]. Presently, PCs have gained the attention of chemists and materials scientists because of the challenges posed by their synthesis, treatment, and characterization. Due to technological advancements and rising demands for porous materials, researchers have developed synthetic methods that allow them to control the parameters that determine structural and textural properties [6,7].

Ring structures with at least one C atom and one or more other atoms are referred to as heterocyclic compounds, which are ubiquitous in nature and find widespread applications in pharmaceutical and medicinal chemistry due to their potent bioactivities (Fig. 1). It has been estimated that more than 85% of all bioactive chemical entities contain a heterocyclic compound. Heterocycles include several biochemicals essential to life. Many naturally occurring vitamins, pigments, hormones, nucleic acids, and antibiotics are heterocyclic compounds. Most pharmaceutical products that mimic natural products with biological activity are heterocyclic compounds [8]. Heterocycles constitute around 50% of known organic compounds, and approximately 90% are active pharmaceuticals. These compounds play a significant role in drug discovery and development; therefore, from a green chemistry perspective; researchers are engaged in designing, and developing novel and green routes for their high-yield synthesis [9].

Over the past decade, the rising credibility of PC catalysis in organic transformations and their outstanding features have stimulated researchers to study their synthesis, properties, and applicability. Consequently, a good number of research papers on the synthesis and applications of PCs in organic transformations were published. Further, based on PCs materials, the following reviews were also reported in the literature. In 2016, Wang *et al.* [10] reviewed N-doped PC catalysts for heterogeneous hydrogenation and oxidations. In 2022, Lin and co-workers [11] reviewed carbohydrate-derived PC catalysts for various organic transforma-

E-mail address: uppatil4143@rediffmail.com

https://doi.org/10.1016/j.cclet.2023.109472
1001-8417/

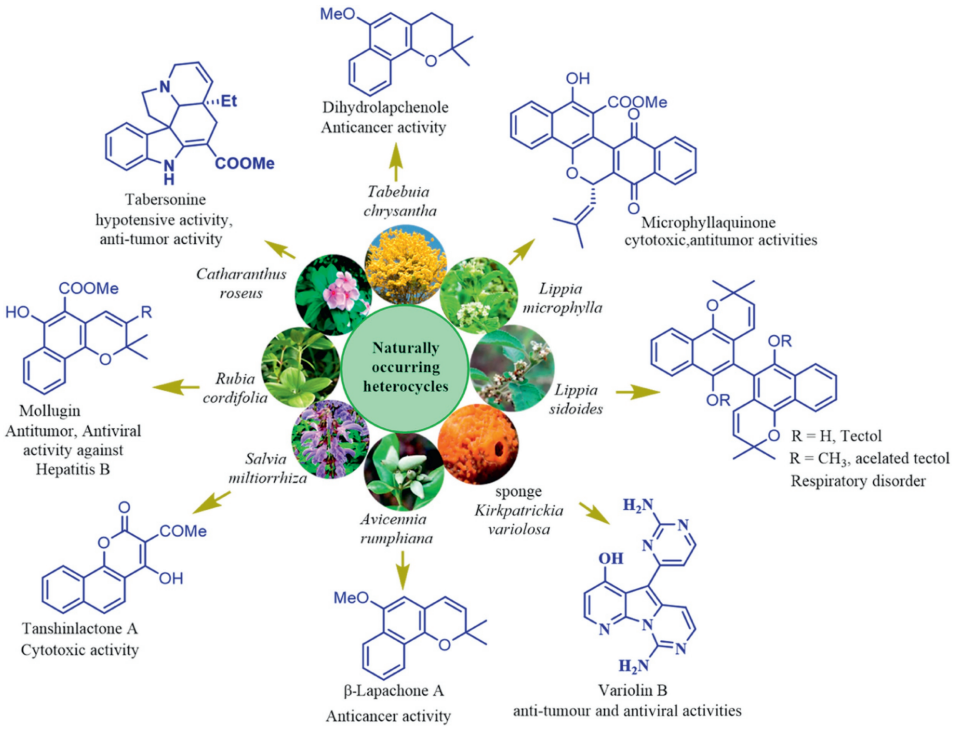

Fig. 1. Glimpse of natural bioactive heterocycles.

tions, in 2015, De *et al.* [12] reviewed biomass-derived PC for organic synthesis as well as electro- and photochemical processes in aqueous solutions while, in 2020, Rai *et al.* [13] reported a review on carbon-based materials such as carbon nanotubes, graphitic nitride, and nitrogenous carbon materials for heterocycle synthesis. In 2019, the Pérez-Mayoral group reviewed PC catalysis in fine chemical synthesis [14], and in 2020, Gläser *et al.* [15] reviewed chitosan-based N-doped carbon materials for photocatalytic and electrocatalytic applications. Rangraz *et al.* [16] in 2021 reported recent advances in heteroatom-doped porous carbon/metal materials and their applications in organic transformations. While, in 2022, Zhang's group reviewed the recent progress in design principles and synthesis methods of asymmetric C- and Si-based nanomaterials and their applications in energy storage, catalysis, and biomedicine [17].

However, in these reviews, few PC-catalyzed heterocyclic reactions have been reported. Considering the inherent advantages of PC catalysts and their increasing applicability, a study on heterocycles synthesis over PC is highly significant and appealing. With this view, economic and environmentally benign processes for synthesizing functionalized heterocyclic compounds using PC catalysts have been widely discussed in this review. Moreover, challenges and opportunities in the field of PCs and their implications in heterocycles synthesis have also been discussed.

2. Advances in the synthesis of porous carbon materials

Various synthetic or natural sources are used for the synthesis of PC materials. PCs can be derived from readily available biomass such as wood, rice husks, coconut shells, fruit pits (*e.g.*, peach pits), nutshells (*e.g.*, walnut shells), seeds (*e.g.*, apricot kernels), and other agricultural waste. Additionally, synthetic polymers such as polystyrene, polyacrylonitrile (PAN), polyvinyl chloride (PVC), phenolic resins, some petroleum-based products, such as petroleum coke, pitch, and refinery residues, as well as metal-organic framework (MOF), covalent organic framework (COF), and organic compounds are used as a source to derive porous carbons [18–23]. Different methods such as physical activation, chemical activation, or a combination of physical and chemical activation, catalytic activation, carbonization of blends (carbonizable polymer and pyrolyzable polymer), polymer aerogel carbonization under supercritical drying conditions, are used for the PCs production.

2.1. Physical activation

The production of PC materials by physical activation is a versatile method to create high-surface-area carbonaceous materials with a network of interconnected pores [24]. Initially, precursors (biomass, polymers, or petroleum derivatives) are selected and carbonized. This process involves heating the material typically between 600 °C and 900 °C. At the time of carbonization, volatile components, such as water, volatile organic compounds (VOCs), and some non-carbon components, are driven off, leaving behind a carbon-rich residue. The resulting residue is ground into a fine powder and sized to the desired particle size distribution. The particle size can influence the porosity of the final product [25]. It is further subjected to partial and controlled gasification at high temperatures using activating agents such as CO_2, steam, air, or a mixture of both. The gasification process selectively removes the most reactive carbon atoms from the structure generating the porosity. Further, gasification will produce the final carbon with a highly porous structure and high specific surface area sought [26]. A pressurized physical activation [27] showed excellent results afforded increased specific surface area (>2600 m^2/g), pore volume, and formation of micropores in carbon compared to atmospheric pressure. Colomba *et al.* [28] reported producing biochar at a higher heating rate contains excessive pores, and under physical activation using a CO_2 activator, the specific surface area (1300 m^2/g) was increased. In a recent report, Pallares *et al.* [29] found that the choice of activator and temperature conditions play a crucial role in preparing PC under physical activation. The CO_2 activator at 800 °C afforded 789 m^2/g of surface area and 0.3268 cm^3/g of micropore volume, while the steam activator at 700 °C offered 552 m^2/g of surface area and 0.2304 cm^3/g of micropore volume.

Physical activation allows for control over the size and distribution of pores in the carbon material and generally produces high-purity carbon materials. This method is often considered more environmentally friendly since it uses benign agents like steam or carbon dioxide, lowers activation costs, is free from chemical waste production, and does not use harsh chemicals. However, physical activation might sometimes be less efficient in creating highly porous structures, and the porosity achieved might be lower or require longer processing times, impacting the overall efficiency of the method. Zaini *et al.* reported that compared to CO_2, steam worked well in developing the matrix with high surface area (2938 m^2/g) and pore volume, but it required higher temperature, longer activation time, and resulting lower yield [30].

2.2. Chemical activation

PCs can also be generated by the chemical activation process. In this process, the precursor is impregnated with activating chemical agents. Generally, activating agents such as KOH, NaOH, K_2CO_3, $ZnCl_2$, H_3PO_4 [31,32] are used. The activating agent is treated with carbon precursor either by direct mixing or using its aqueous solution [33]. After impregnation, the chemical activation procedure is performed in an inert atmosphere under various temperature conditions (400–900 °C) depending on the type of activating agent used [34]. Activating agents restrict the formation of tars, VOC, and bitumen, and help increase the well-developed porous carbon contents [35]. These agents play a significant role in the formation of tiny pores in the carbon skeleton that lead to an increase in the specific surface area. Chemical activation is more economical as compared to physical activation, because it is performed at lower activation temperature, requires a short processing time, and it offers highly porous carbon with more efficiency [36]. However, the use of chemical activating agents can leave residues in the PC material, potentially affecting its purity. This process involves the removal of carbon atoms to create pores, leading to a loss in PC yield [37].

The physicochemical activation (combination of physical and chemical activation) involves the carbonization of a chemically impregnated raw precursor followed by a physical activator or the carbonization and activation of chemically impregnated char with oxidizing gas or steam. This method produces a carbon skeleton with higher surface area and pore volume than individual activation due to improved mass transfer with carbon matrix [38]. Adlak *et al.* [39] used both chemical (KOH) and steam (physicochemical activation) activators for the preparation of PCs from neem (*Azadirachta indica*) wood as a carbon precursor. This method resulted in a higher specific surface area (963 m^2/g) and porosity compared to chemical activation. While physicochemical activation has several advantages such as PCs with high surface area and porosity, there are also some disadvantages including higher energy consumption during the synthesis process, chemical waste generation, formation of undesirable by-products, longer activation time, and sometimes chemical agents may remain in carbon matrix which could inhibit pore formation [40].

2.3. Heteroatom doping methods

The introduction of heteroatoms (N, P, S, O, B, *etc.*) into the carbon skeleton can significantly enhance the performance of PC materials for various applications [41]. After selecting a proper carbon precursor, heteroatoms can be introduced into carbon lattice using various techniques. By the chemical vapor deposition method, heteroatom-containing gasses like ammonia, nitrogen oxide, sulfur-containing gases, are introduced during the carbonization process, leading to the incorporation of heteroatoms into the carbon structure [42]. In the chemical modification method, after carbonization, the PC material can be chemically treated with heteroatom-containing reagents to functionalize the surface [43]. Using the co-pyrolysis method, heteroatom-containing reagents are mixed with carbon precursor and then subjected the mixture to pyrolysis [44]. This allows for the incorporation of heteroatoms during carbonization. In wet chemical method, dopant precursors in solution are infiltrated into the PC material, and then heat treatment is applied to remove the solvent and incorporate dopant atoms [45]. Template-assisted method can also be used for doping heteroatom into PC material. High-energy ions of the dopant element are accelerated and implanted into the carbon skeleton. Subsequent annealing or heat treatment helps to stabilize the dopant atoms in the lattice. Zhang *et al.* [46] prepared two kinds of highly N-doped mesoporous carbon onto nanotubes (NMC/CNTs) based on a facile cooperative assembly process assisted by triblock $PEO_{20}PPO_{70}PEO_{20}$(P123) and $PEO_{106}PPO_{70}PEO_{106}$ (F127) copolymers. Wang *et al.* [47] recently developed a composite material consisting of Co NPs and single atom Zn co-implanted in N-doped PC nanosheets grafted with carbon nanotubes (CNT). Jiao and co-workers [48] reported single atom Fe implanted N-doped PCs *via* pyrolysis (Fig. 2). Heteroatom doping in PC offers several advantages, including enhanced catalytic activity, improved conductivity, and altered surface chemistry. However, limitations of this method include the complexity of synthesis, sometimes non-uniform distribution, increased cost, and some metals used for doping may have toxicity concerns that can cause health and environmental issues.

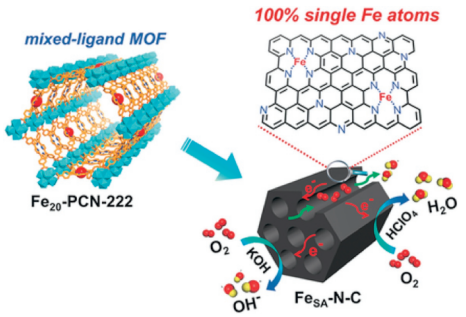

Fig. 2. Pyrolysis of porphyrinic MOF to afford high content single-atom Fe-implanted N-doped PC. Reproduced with permission [48]. Copyright 2018, Wiley-VCH.

2.4. Metal-catalyzed activation method

This method typically involves the use of carbon precursor (polymers like phenolic resins, polyacrylonitrile (PAN), organic compounds, cellulose, lignin, and various biomass-derived materials) and a transition metal catalyst (iron, nickel, cobalt, *etc.*) to create porous structure through a combination of carbonization and activation process. The choice of precursor can impact the properties of the resulting PC. Initially, a catalyst is introduced into the carbon precursor, and the mixture is heated at a high temperature in an inert atmosphere. The catalyst promotes the formation of carbonaceous structures by fascinating the removal of VOC and creating voids in the carbon matrix [49–51]. Although catalytic activation remains a valuable method for producing PC materials with tailored properties for a wide range of applications, the chemical residue of catalytic material may be incorporated in the final PC materials, which can affect the product purity, and yield. Achieving uniform dispersion of the catalyst within the carbon precursor can be challenging. Non-uniform distribution can result in uneven pore formation and material's properties inconsistencies.

2.5. Templating methods

Since the last decade, various templating methods such as hard template, soft template, and self-templating have emerged as suitable alternatives to traditional methods. In the hard templating method, ordered inorganic porous solids such as mesoporous silica, zeolite, clay materials, can be used. Hard templating is a multifarious process involving: (1) Template preparation under controlled porosity; (2) introducing carbon precursor in the template pores; (3) cross-linking and carbonization of the carbon precursor to create organic-inorganic composites, and finally, (4) removal of the inorganic constituents to get a PC material [12]. For hard-templating, the use of inorganic materials such as oxides (MgO, ZnO, MnO_2, iron oxides, *etc.*), salts (NaCl, KCl, $CaCO_3$, Na_2SO_4, *etc.*), and metals (Zn, Fe) are advantageous over silica, because they are abundant, non-toxic, an economic, and easily removable with diluted acids or water, avoiding toxic HF [52].

In the soft templating method, the surfactant (trimethylstearylammonium chloride, sorbitan monooleate, perfluorobutane sulfonate, sodium dodecylsulfate, tetrapropylammonium bromide, pluronic F-127, Triton X-100, pluronic P-123, *etc.*) is mixed with the carbon precursor, either using water or ethanol, that undergoes spontaneous micellation. These micelles may be layered, spherical, cylindrical, or ellipsoidal as per the molecular geometry of the surfactant and the dilution conditions (surfactant concentration, pH, *etc.*). Further polymerization and cross-linking of the carbon precursor leave the micelles trapped in a continuous polymeric matrix. A high temperature causes carbonization of the polymer and complete removal of surfactant, yielding mesoporous carbon material [53,54]. In hydrothermal carbonization, the precursor of the carbon is gradually hydrolyzed, dehydrated, condensed, and aromatized under high temperature and pressure using water as a solvent and finally converted into PC material [55]. In a self-generated templating approach, carbon precursors can directly be carbonized to obtain PCs. In some cases, the cation or anion of the ionic liquids can be used as pore-forming agents without any other scaffold. This approach avoids the waste and pollution caused by using templating agents. However, solid carbon precursors are difficult to achieve self-assemble, or produce pore-forming agents during carbonization [56].

Besides, mechanochemically-assisted templating is also a promising alternative to the traditional method because this method reduces solvent consumption and waste generation. Solventless synthesis of PC can be performed by mixing organic compounds like resorcinol, terephthalaldehyde, and block copolymer (F127). Grinding of this mixture for 5 min. produces a sticky paste-like mixture. After the carbonization of this mixture, PCs with cubic and hexagonal structures are obtained [57,58]. Zhang *et al.* [59] have ingeniously designed B,N co-doped hierarchically PC nanosheets (BNPC) *via* a hard-templating route and simple carbonization process. The hard-templating method can synthesize homogeneous pores and ordered pore structure carbon with a high specific surface area. However, this method is more complicated, not cost-efficient, and needs a relatively long synthesis time [51,56].

The process of carbonizing polymer blends is also used in the production of PCs. This involves blending a carbonizable polymer (such as phenolic resins, aromatic polyurea, polyacrylonitrile (PAN), pitch-based polymers) with a pyrolyzable polymer (such as polyvinyl chloride (PVC), polystyrene, polyethylene) having variable degrees of thermal stability. The blend is then carbonized at high temperatures in an inert atmosphere. During the process, the pyrolyzable polymer is completely eliminated in pyrolysis, leaving pores in the carbon skeleton of the carbonizable polymer. The blending ratio of the component polymers can be adjusted to control the pore volume and size in the final PC [49]. However, volatile organic compounds (VOC) or other potentially harmful substances may be released during the process, so environmental controls and proper safety measures are necessary to mitigate these concerns. The carbonization of organic aerogels is one more method employed to produce PC materials. Organic aerogels are synthesized through the sol-gel process, where a liquid precursor undergoes gelation to form a three-dimensional network structure. This gel is then subjected to supercritical drying or freeze-drying to remove the liquid component while retaining the aerogel's porous structure. The organic aerogel is then carbonized at high temperatures in an inert atmosphere. The resulting carbon material retains its high specific surface area and innate porosity. Careful control of the carbonization conditions may be required to achieve specific pore structures and size distributions [60–62].

3. Synthesis of functional heterocycles using porous carbon catalysts

Functionalized heterocyclic compounds have enormous importance in pharmaceutical and medicinal chemistry because of their potential biological activities. They are frequently found in biomolecules such as vitamins, enzymes, pigments, hormones, and many natural products [8]. Owing to their medicinal significance, several attempts have been made to synthesize these compounds using homogeneous and heterogeneous catalysts [63–70]. PC catalysts are heterogeneous solid materials with high specific surface area, dispersion ability, thermal stability, and reusability, and more significant is that PC is a cost-effective and environmentally friendly catalytic system. Due to these striking features, PC is more advantageous over stoichiometric reagents or homogeneous catalysts. PC-catalyzed synthetic methods reported in the literature are examined and compiled as under.

3.1. Oxidation

The saturated or partially saturated heterocyclic compounds offer an efficient and straightforward route for the synthesis of functional *N*-heterocycles *via* oxidative dehydrogenation reactions [71]. With this view, in 2022, Sun and co-workers [72] developed N,P-co-doped carbon material (NPCH) and employed it in the oxidative dehydrogenation of derivatives of 1,2,3,4-tetrahydroquinoline **1** into the quinoline **2**, indoline **3** into the 1*H*-indole **4**, and other *N*-heterocycles (Scheme 1). For the catalyst preparation, in the aqueous mixture of 2-methylimidazole and benzylamine, $Zn(NO_3)_2{\cdot}6H_2O$ was added and stirred at room temperature to get ZIF-8-Bn. It was mixed with PPh_3 and pyrolyzed at 900 °C in an N_2 atmosphere to produce a catalyst. At the time of pyrolysis, Zn species were evaporated. Further, for the complete removal of Zn species, the catalyst was treated with HCl. Due to the removal of Zn species, the defects in the catalyst were developed.

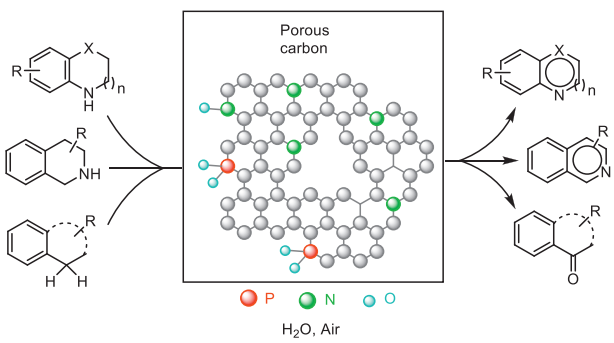

Scheme 1. N,P co-doped PC catalyzed oxidative dehydrogenation of *N*-heterocycles.

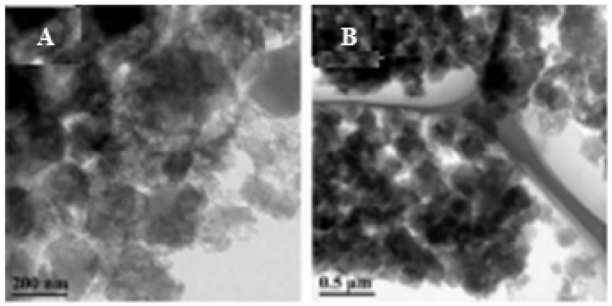

Fig. 3. TEM images of (A) NPC-300 and (B) NPCH catalysts. Reproduced with permission [72]. Copyright 2022, Royal Society of Chemistry.

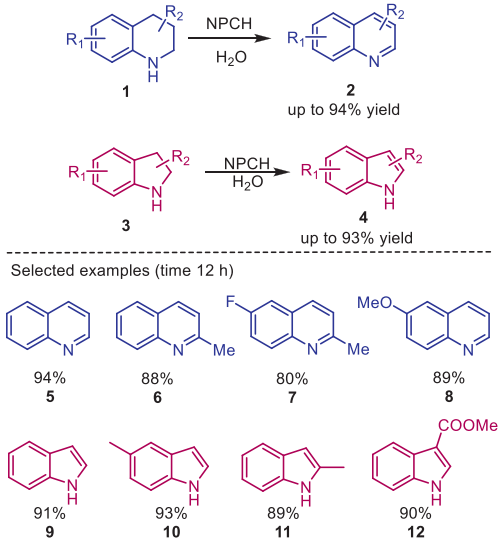

Scheme 2. Oxidative dehydrogenation using N,P co-doped PC catalyst.

Analytical tools such as XRD and Raman spectra of the catalyst exhibited graphitic features and structural defects, TEM images (Fig. 3) showed that the average particle sizes of NPC-300 and NPCH are 182 nm and 180 nm, respectively, while elemental mapping revealed the homogeneous dispersion of C, N, O, and P species over the entire nano-architecture, and XPS analysis confirmed that N and P heteroatoms were successfully doped in PC.

The active sites such as P, and N centers, which are possibly responsible for dehydrogenation, offer heteroarenes with high selectivity (Scheme 2). Furthermore, two pharmaceutically relevant molecules such as 6-((2-(dimethylamino)ethyl)amino)−3–hydroxy-7*H*-indeno[2,1-*c*]quinolin-7-one **15** from 6,6*a*,7,11*b*-tetrahydro-5*H*-indino[2,1-*c*]quinoline **13**, and (*R*)−2-(1-((4-(4-fluorophenyl)quinolin-7-yl)methyl)−1*H*-1,2,3-trizol-4-yl)butan-2-ol compound with trifluoro-λ^3-methane (1:1) **18** from 4-(4-fluorophenyl)−1,2,3,4-tetrahydroquinoline **16** have been synthesized using PC catalyst, which signifies its importance (Scheme 3). A gram-scale synthesis indicates the industrial applicability of the catalyst. Although the developed NPCH catalyst is good enough to offer up to 94% yield and is reusable, the leaching of Zn species and the use of acid for its complete removal from the catalyst can raise environmental issues. To overcome this problem, Zn species can be recollected and reused.

As an alternative to precious metals and a very efficient dehydrogenation catalyst, activated carbon (Darco KB) has been employed by Krivec and co-workers [73] for the synthesis of a set of novel isoindoles **21** *via* a one-pot Diels-Alder reaction in decalin solvent at 180 °C that offered up to 87% yield (Scheme 4). In the preparation of isoindole derivatives from the reaction of *N*-

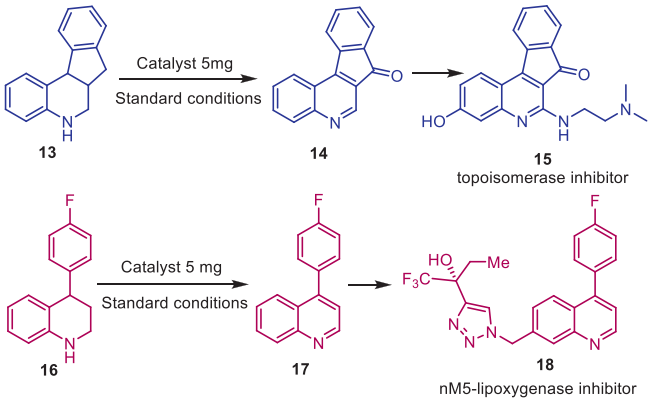

Scheme 3. Synthesis of bioactive compounds using N,P co-doped PC catalyst.

substituted maleimides **19** with 2*H*-pyran-2-ones **20** *via* cycloaddition/elimination/dehydrogenation, the catalyst influences the dehydrogenation, which is essential to avoid the formation of a possible product bicyclo[2.2.2]octenes. It is also proven that the aromatization occurs *via* hydrogen transfer facilitated by a heterogeneous carbon catalyst from the cyclohexadiene intermediate to the maleimide derivative. Compared to the BET surface area of Rh/C (832 m^2/g) and activated carbon (700 m^2/g), Darco KB has a significantly higher specific surface area (1320 m^2/g). The effective surface functionality of the Darco KB catalyst possibly enables more efficient facilitation of the dehydrogenation process. The method is advantageous because it avoids the use of expensive noble metals, and offers up to 87% yield of the products; however, the solvent effect on the product yield is not considered.

Su and co-workers [74] reported the synthesis of quinazolinones **28** *via* a tandem hydrogen-transfer strategy catalyzed by N,S codoped carbon-anchored Co NP. The catalyst N,S-codoped carbon-anchored Co NP (Co@NSC-1) was developed by the pyrolysis of a mixture of Co/Zn-zeolitic imidazolate framework and thiourea. Quinazolinones **28** were synthesized from 2-nitrobenzonitrile **26** and benzyl alcohol **27** using a Co@NSC-1 catalyst that offered up to 98% yield (Scheme 5). The superior performance of the Co@NSC-1 catalyst is attributed to the uniform dispersion of Co NPs, a high specific surface area, potent acid-base sites, and synergistic effects between Co NPs and N,S-dopants so that it exhibited no significant loss in activity after the 6th run, and afforded a high yield (98%) of the product compared to the previously reported methods.

Liu's group [75] prepared N-doped PC and employed it in the aerobic dehydrogenation of *N*-heterocycles. Sugarcane bagasse was used as a source for the PC generation. The TEM, N_2-sorption, XPS, and EPR analysis revealed that the increased catalytic properties of NC resulted from its high activation ability for both O_2 and heterocyclic N. The developed PC had graphene-like surface morphologyand a well-developed porous structure and was found to be highly active toward the dehydrogenation of *N*-heterocycles. The protocol offered up to 96% yield of the desired products (Scheme 6). This method boasts waste-derived and reusable catalysts, ethanol as a green solvent, requires minimal energy input, and produces high yields, making it both cost-effective and environmentally friendly.

For the preparation of bio-derived aromatic polyesters, the oxidation of HMF **29** to 2,5-furandicarboxylic acid (FDCA) **30** under suitable experimental conditions is a sustainable and promising method. With this view, Yang *et al.* [76] developed Pt/NC-800 catalyst and successfully employed it for the aerobic oxidation of HMF **29** to FDCA **30** using Na_2CO_3 base at 110 °C with 100% conversion (Scheme 7). *N*-Doped carbon catalyst was prepared by pyrolysis of natural carbon resource pomelo peel at 800 °C under

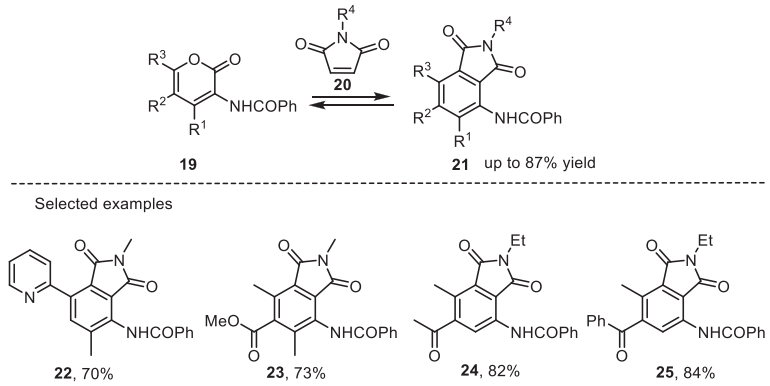

Scheme 4. Synthesis of isoindole derivatives using activated carbon (Darco KB).

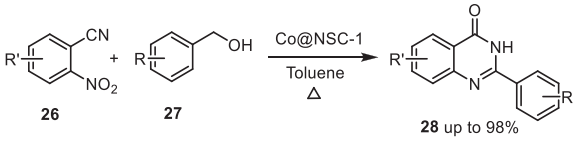

Scheme 5. Synthesis of quinazolinones using Co@NSC-1 catalyst.

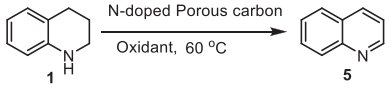

Scheme 6. Aerobic dehydrogenation of *N*-heterocycles.

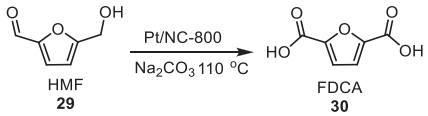

Scheme 7. Pt/NC-800 catalyzed aerobic oxidation of HMF into FDCA.

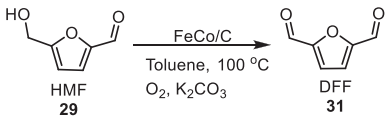

Scheme 8. Aerobic oxidation of HMF to DFF using FeCo/C catalyst.

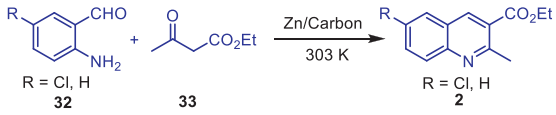

Scheme 9. ZnO/carbon catalyzed synthesis of quinolines.

NH_3 (Nitrogen source up to 11.4%) flow with a uniform dispersion of Pt-NPs. The developed catalyst was characterized by analytical tools. Warped carbon nanosheets (calcined above 800 °C) formed web structures deduced by SEM images. The XPS analysis showed Pt nanoparticles (NPs) are supported on NPC-800, while the XRD pattern ascribed crystalline planes of supported Pt nanoparticles (NPs). The N_2-sorption experiments showed a large surface area (513.3 m^2/g to 809.2 m^2/g), pore volume (220.9 cm^3/g to 331.9 cm^3/g), and pore diameter (0.32 nm to 0.47 nm). These textural properties could be responsible for catalytic activity enhancement. Though the method is opportune due to the use of waste material as a carbon source, and a high N-contentsin the catalyst, the use of expensive Pt affects the overall cost of the method.

Carbohydrate-derived HMF **29** is a precursor of 2,5-diformylfuran (DFF) **31** intermediate compound, which is useful for the synthesis of pharmaceuticals, fluorescent material, fine chemicals, surfactants, and others [77–79]. Fang *et al.* [80] developed hollow magnetically separable FeCo/C nanocatalyst and employed it in the selective oxidation of DFF **31** from HMF **29** that afforded >99% yield under mild reaction conditions (Scheme 8). A hollow magnetically separable FeCo/C catalyst was prepared by thermolysis of a bimetallic MOF (MIL-45b) containing non-noble metals Co and Fe. In the catalytic characterization, XRD showed a crystalline nature, SEM micrograph revealed irregular agglomerates, XPS spectra indicated the presence of Fe^{3+} and Co^{4+} species in the catalyst, and TEM images exhibited a hollow nature of FeCo/C-500 Nps. The hollow structural appearance of FeCo/C nanocomposite material favored the adsorption of HMF **29** and rapid desorption of product DFF **31** from the catalyst surface with a high yield. The catalyst could be reused up to the 6^{th} cycle without significant loss in activity. FeCo/C nanocatalyst demonstrated superior performance for HMF oxidation compared to other catalysts, as shown in Table 1 [80–84] in sequence. This protocol utilizes low-cost and magnetically separable transition metals instead of noble metals, which were highly active and selective toward HMF oxidation, resulting in >99% yield of the product.

Quinolines **2** are present in several natural and synthetic products endowed with biological activities [85]. Classical Friedländer condensation is the simplest and most effective route among several methods for the synthesis of quinolines **2**. In general, Friedländer condensation is considered an atom-efficient reaction that proceeds through double condensation between 2-aminoaryl carbonyl compounds with other carbonyl components possessing active methylenic units at α-position affording quinolines. For the synthesis of quinolines **2** *via* Friedländer condensation reactions, different PC-based catalytic systems were employed that showed quite efficient catalytic performance [86].

ZnO/carbon nanocomposites [87] exhibited excellent catalytic activity towards the synthesis of quinolines, *via* Friedländer reaction, from 2-amino-5-chlorobenzaldehyde **32** and ethyl acetoacetate **33** under solventless conditions (Scheme 9). Zn-containing various catalytic materials such as Norit1Zn (activated carbon support), CNT_{OX}3Zn, Z1200 (MOF Basolite®), and SBA15–3 Zn (silica-supported catalyst) were well-examined using various analytical tools. The influence of the physicochemical properties of various carbon supports, such as activated carbon (AC), carbon aerogel (CA), and multi-walled carbon nanotubes (MWCNT), on the catalytic performance was also investigated. The authors stated that catalytic support is a key factor in the development of new catalysts with enhanced properties. Comparatively, the Norit1Zn is more active than other Zn-containing catalysts such as commercial MOF or ZnO-supported on SBA-15 mesoporous silica (even 3-fold higher Zn content). The outstanding catalytic performance for

Table 1
Comparative results of HMF oxidation.

Catalyst	HMF concentration (mol/L)	Metal loading (mol%)	Temp. (°C)	P(MPa), atmosphere	DFF yield (%)	Ref.
Ag-OMS-2	0.063	16.7	165	1.5, air	99	[81]
Pd/C	0.067	2.5	80	2.0, O_2	8.8	[82]
Pt/C	0.067	2.5	80	2.0, O_2	1.3	[82]
γ-Fe_2O_3@HAP-Ru	0.11	3.7	110	0.1, O_2	81	[83]
Ru/HT	0.33	4.3	120	0.1, O_2	92	[84]
FeCo/C(500)	0.50	20	100	1.0, O_2	>99	[80]

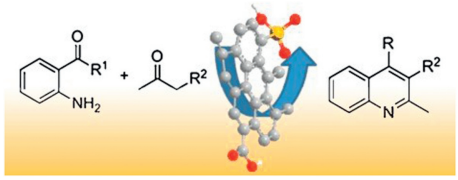

Scheme 10. Acid-activated carbon catalyzed synthesis of substituted quinolines. Reproduced with permission [88]. Copyright 2013, ChemCatChem.

Norit1Zn in the synthesis of quinolines **2** probably associated with the accessibility of active catalytic centers. Friedländer condensation of carbonylic compounds with 2-amino-5-chlorobenzaldehyde and enolizable hydrogens using Zn/carbon catalyst under solventless and mild reaction conditions, at lower temperature, affording in all cases selectively a total conversion to the corresponding quinolines.

In another experiment, series of activated carbons (ACs) such as mesoporous carbon (Cmeso), activated mesoporous carbon (ACmeso), microporous carbon, Norit/N, Norit/S, Merck/N, and Merck/S were synthesized, characterized, and tested for the synthesis of quinolines **2** (Scheme 10) *via* Friedländer reaction by Pérez-Mayoral group [88]. The authors reported that from the characteristic study of the various carbon-based catalysts, Norit/S catalyst containing sulfonic acid groups with the highest surface area has higher acidity than other catalysts and exhibited an excellent performance towards condensation reaction. The reaction of 2-aminobenzophenone and ethyl acetoacetate **33**, and the reaction of 2-aminoaryl ketone with acetylacetone catalyzed by Norit/S at 363 K offered 98%, and 92% conversion respectively, compared to other catalysts. Ease of catalyst preparation from commercial microporous materials, its tunable acidity, and affording quinolines with high conversion and mild reaction conditions are the remarkable features of this method.

A hierarchically PC-supported single-atom catalyst (SACs) was developed by Chen and co-workers [89] and was used to synthesize quinoline derivatives **36** *via* Friedländer condensation (Scheme 11). The catalyst was prepared following a top-down approach. Natural birch wood was treated with metal salts ($FeCl_3$, $CoCl_2$, $NiCl_2$, or $CuCl_2$), and after pretreatment; the hydrothermally treated wood was carbonized (Fig. 4). In this process, wood was used as a carbon source, while urea as a nitrogen source. Fe-single atom PC catalyst calcined at 800 °C referred to as Fe-800 SAC.

The catalyst was well-characterized using various techniques. SEM images (Fig. 5) revealed a microporous structure with a diameter of 1020 µm. N_2-sorption illustrated a BET area of 164 m^2/g and pore size of 3.8 nm, while uniform dispersion of N and Fe in the carbon skeleton was deduced by elemental mapping. The doping of N was confirmed by XPS analysis. Raman, FTIR, and NMR spectra exhibited the presence of defective sites and functional groups, while Mössbauer spectra indicated the presence of Fe species. Fe-800 SAC was employed for the synthesis of quinoline derivatives **36** by oxidative cyclization of aniline **34**, and acetophenone **35** derivatives at 120 °C in DMSO under an O_2 atmosphere

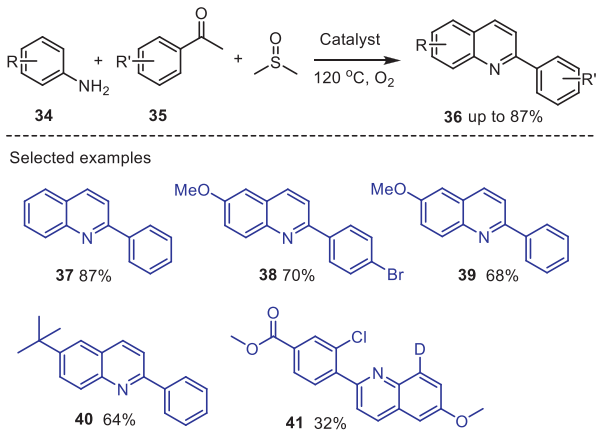

Scheme 11. SAC-catalyzed oxidative cyclization.

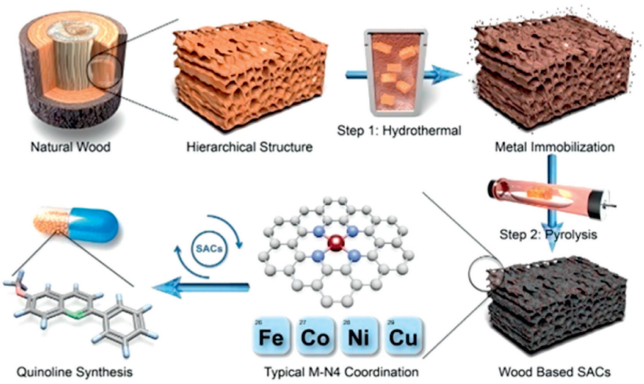

Fig. 4. Preparation of wood-based single-atom PC catalyst and its applications. Reproduced with permission [89]. Copyright 2021, Wiley-VCH.

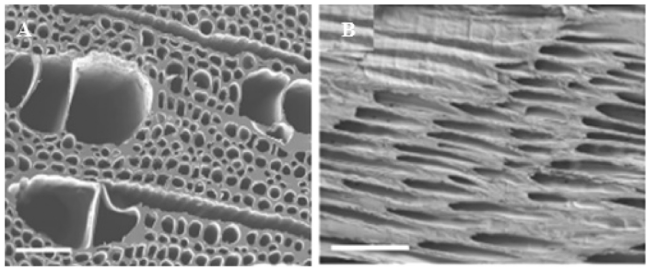

Fig. 5. SEM images of (A) Fe-800 SAC and (B) Fe-800 SAC along the parallel direction. Reproduced with permission [89]. Copyright 2021, Wiley-VCH.

that offered up to 87% yield. Moreover, oxidative dehydrogenation of **1** and synthesis of methyl 3–chloro-4-(6-methoxyquinolin-2-yl)benzoate **41** a building block of cavosonstat (inhibit the *S*-nitrosoglutathione reductase (GSNOR) enzyme), were carried out using the catalyst at 120 °C under air. A low-cost transition metal and wood material as a carbon source was used to develop the

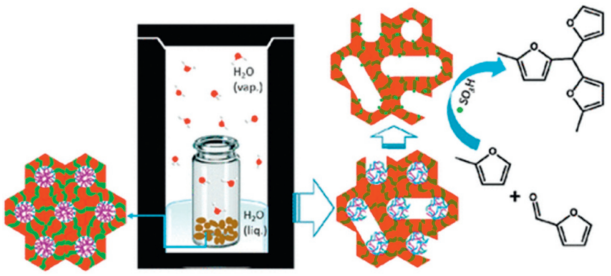

Scheme 12. Synthesis of sulfonated mesostructured silica-carbon nanocomposite catalyst and its application in the synthesis of FMBM. Reproduced with permission [91]. Copyright 2018, American Chemical Society.

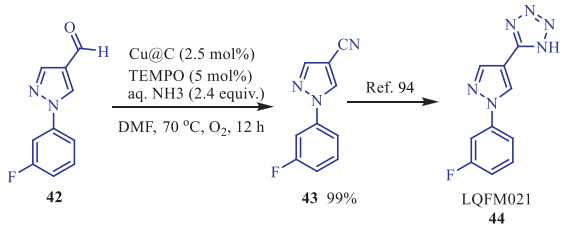

Scheme 13. Synthesis of biologically active compound using Cu@C/TEMPO catalyst.

catalyst (SAC). Such PC-supported SACs exhibited excellent activity and selectivity toward oxidative dehydrogenation of THQ as well as the construction of substituted quinolines by oxidative cyclization compared to PC-supported noble metals. Hence, this protocol is both cost-effective and environmentally friendly.

2,2′-(2-Furylmethylene)bis(5-methylfuran) (FMBM) heterocycle is an important precursor for biodiesel production [90]. With this view, Sels and co-workers [91] have developed sulfonated mesostructured silica-carbon nanocomposite ($Si_{33}C_{66}HTSO_3H$) catalyst for the solvent-free synthesis of 2,2′-(2-furylmethylene)bis(5-methylfuran) from condensation reaction of sylvan (2-methylfuran) and furfural at 50 °C with 86% product yield and 90% selectivity (Scheme 12). The mesostructured silica-carbon nanocomposites with extensive mesopore interconnectivity developed from sucrose as a carbon source using a mild vapor-phase-assisted hydrothermal treatment procedure. The resultant nanocomposite materials were sulfonated to get strong acid catalysts. These catalytic materials were well-characterized by SEM, TEM, TGA, SAXS, NMR, Raman, N_2-sorption, XPS, *etc.*, which clearly demonstrated the formation of catalysts. The superior catalytic performance is due to higher carbon content, SO_3H density, the presence of more open interconnected mesopores in Si-C nanocomposites, and higher oxygen functionality.

The catalyst offered an excellent yield of the desired product without the formation of hydroxyalkylation or other intermediates. The catalytic recyclability test showed that after the 2nd run, the catalytic activity was significantly reduced, however, with regeneration by resulfonation, the catalyst showed excellent performance in the subsequent run.

The pyrazole derivative 5-(1-(3-fluorophenyl)−1*H*-pyrazol-4-yl)−2*H*-tetrazole (LQFM-21) **44** exhibits antinociceptive, vasorelaxant, and anti-inflammatory activities [92]. In addition to the aerobic oxidative conversion of benzaldehyde into benzonitrile using a heterogeneous copper catalyst (Cu@C)/TEMPO, Yoon *et al.* [93] have also synthesized 1-(3-fluorophenyl)−1*H*-pyrazole-4-carbonitrile **43**, an intermediate compound in dimethylformamide at 70 °C that offered 99% yield (Scheme 13). Further, LQFM021 **44** was synthesized following Zang's protocol [94]. The catalyst Cu@C was developed by the pyrolysis of HKUST-1, which showed good catalytic activity and reusability up to the 3rd cycle.

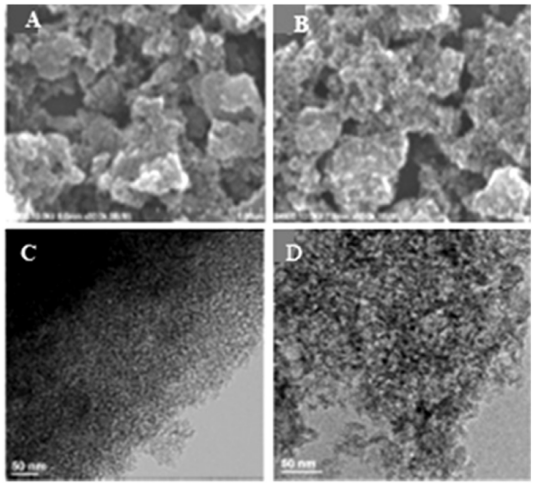

Fig. 6. SEM images (A, B), and TEM images (C, D) of the porous carbon materials. Reproduced with permission [95]. Copyright 2021, American Chemical Society.

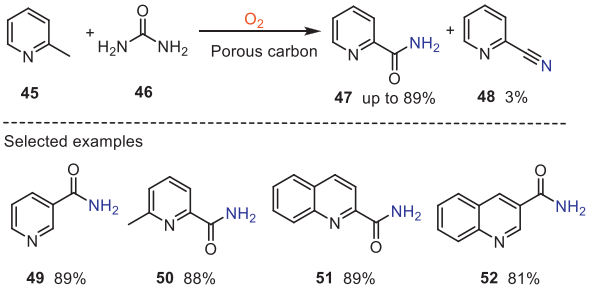

Scheme 14. PC-catalyzed direct oxidative amination of *N*-heterocycles.

The direct oxidative amination of the methyl C−H bond in N-heterocyclic compounds to prepare the corresponding amides using a PC catalyst has been reported by Long and co-workers [95]. Non-doped, N-doped, and P-doped PCs were synthesized. A PC catalyst was synthesized by hard template method using silica nanospheres and sucrose as a carbon source carbonized at 900 °C, by treating this mixture with HF for removal of silica. Similarly, N-doped and P-doped PCs (cyanamide for N and phytic acid for P source), were synthesized using sucrose as a carbon source under various reaction conditions. In catalytic characterization, SEM images (Figs. 6A and B) of PC materials showed the appearance of spongy carbon materials with pores, which indicated SiO_2 hard template successfully directed the formation of pores. It was also supported by TEM (Figs. 6C and D). The HR-TEM images demonstrated the formation of graphene-like layers on the external surface of the carbon. Uniform dispersion of C, N, O and C, P, O in the carbon framework was shown by EDS and XPS. The presence of disordered and graphitic sp^2 carbon was indicated by Raman spectra, XRD exhibited a disordered structure with very low crystallinity, while N_2-sorption showed that the BET surface area of all synthesized PCs ranged from 704 m^2/g to 780 m^2/g and the total pore volume ranged from 1.06 m^3/g to 1.75 m^3/g indicating that C–O is a microporous material. The non-doped PCs exhibited excellent catalytic activity in the synthesis of picolinamide **47** from 2-methylpyridine **45** and urea **46** with up to 89% yield (Scheme 14).

Benzodiazepines **55** are bicyclic compounds possessing two nitrogen atoms at 1- and 5-positions of the seven-membered ring fused to a benzene ring. These bioactive heterocycles are widely used as anxiolytics, CNS depressants, anti-convulsive drugs, hypnotic agents, analgesics, and anti-inflammatory drugs [96,97].

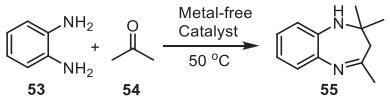

Scheme 15. Synthesis of benzodiazepines.

Godino-Ojer *et al.* [98] reported the synthesis of benzodiazepines **55** from *o*-phenylenediamine **53** and acetone **54** using a metal-free acidic PC catalyst under mild reaction conditions (Scheme 15). In the catalyst preparation, RESOL was used as a carbon precursor. Ethanolic solutions of RESOL and Pluronic F-127 were mixed, dried, and carbonized to get ordered mesoporous carbon (OC). Further, OC, commercially available carbon (N) and xerogel mesoporous carbon (X) were treated with acids (HNO_3 or H_2SO_4), and the resulting acidic carbon materials were used as catalysts. Catalytic materials were well-characterized using SEM, TEM, XPS, TPD, N_2-sorption, and elemental analysis, which showed that both the acid strength and porosity are the main factors influencing the catalytic performance. HNO_3-treated carbon materials showed 100% conversion values at 50 °C after 4 h. The acidic functional groups on the carbon surface can be susceptible to chemical attack, which may limit their applicability in certain industrial processes or applications where chemical stability is crucial.

3.2. Reduction

The addition of hydrogen molecules is an atom-efficient and essential process in organic transformations. This process plays a key role in the synthesis of many functional heterocycles. THQ **1** is an important intermediate for the synthesis of drugs, dyes, alkaloids, agrochemicals, and several other bioactive molecules. For the synthesis of THQ **1**, many methods have been reported, among which direct selective hydrogenation of quinoline is a more convenient and promising method because of its high atom utilization together with easy access to the raw materials [99,100]. Wang and co-workers [101] employed a single Ru site anchored on N-doped PC (Ru SAs/N–C) catalyst for the chemoselective hydrogenation of functionalized quinoline **2** with >99% selectivity (Scheme 16). For hosting Ru atoms, MOF UiO-66 ($Zr_6O_4(OH)_4(BDC)_6$) (BDC = 1,4-benzenedicarboxylate) was chosen due to its outstanding features. To stabilize the $RuCl_3$, the uncoordinated $-NH_2$ located at the terephthalic acid linkers in UIO-66-NH_2 was used. Due to the strong interaction between lone pair electrons and d-orbitals, Ru single atoms would be confined in MOF pores and avoid their aggregation during pyrolysis. As a result, these differently assembled Ru catalysts have excellent catalytic properties toward the hydrogenation of quinoline **2** into THQ derivatives and reusability retained after the 5th run. No doubt the RuSAs/NC catalyst plays a crucial role in the hydrogenation of quinoline derivatives, however, since it utilizes the noble metal Ru, the economic feasibility of the method needs to be considered.

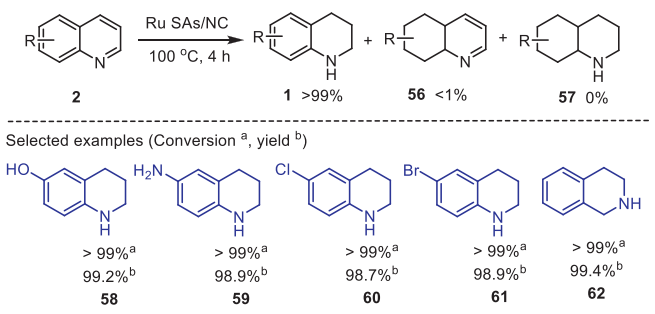

Scheme 16. Hydrogenation of quinolines using Ru SAs/N–C catalyst.

Table 2
Pd-based catalysts performance for selective hydrogenation of quinoline.[a]

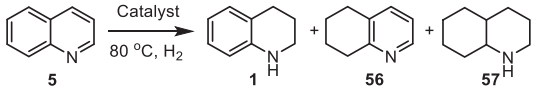

Entry	Catalyst	Conversion (%)[b]	Selectivity (%)[b]		
			1	56	57
1	Pd/C	83.0	>99	0	0
2	CIL-900	0.00	0	0	0
3	Pd@IL-900	26.1	>99	0	0
4	Pd@C-900	90.5	98	2	0
5	Pd@CIL-900-w/o KZ	10.6	91	9	0
6	Pd@CIL-600	81.0	>99	0	0
7	Pd@CIL-700	85.4	>99	0	0
8	Pd@CIL-800	88.3	>99	0	0
9	Pd@CIL-900	97.9	>99	0	0

[a] Reaction conditions: 1.0 mmol quinoline, 0.6 mol% catalyst, 6.0 mL CH_3OH, 1 atm H_2, 80 °C, 4 h.
[b] The conversion and selectivity were determined by GC or GCMS, the by-product is 5,6,7,8-tetrahydroquinoline.

Zhang *et al.* [102] developed N-doped hierarchical PC-anchored tiny Pd NPs (Pd@CIL-900) catalyst and employed in the selective hydrogenation of quinoline **2** under extremely mild conditions. Prepared nitrogen-rich1–butyl–3-methylpyridine dicyanamide ionic liquids (BMPdca ILs), chitosan as composite precursors, and KCl: $ZnCl_2$ salts as pore-forming agents were ball milled, and the obtained mixture was pyrolyzed at 600–900 °C in N_2 gas (Scheme 17). From the synthesized series of catalysts, the carbonized material at 900 °C exhibited the best performance toward selective hydrogenation of quinoline **2** heterocycles with 97.9% conversion and >99% selectivity (Table 2).

The formation of a 3D-hierarchical porous N-doped carbon framework, good crystallinity, uniform dispersion of C, N, and Pd, the Pd NPs diameter (2.5 ± 0.6 nm) a high surface area (1232 m^2/g), pore volume (1.28 cm^3/g), and pore diameter (0.6, 3.7, and 34.5 nm) are the characteristic features resulted from various analytical tools demonstrated the formation of the Pd@CIL-900 catalyst. Notably, a catalyst with high surface area and rich porosity, reusability with good activity, and selectivity up to the 5th run showed that this carbonaceous material could be an appropriate alternative to the traditional catalysts (Pt-, Ru-, Ir-, Rh-based catalysts, which suffer from catalytic poisoning due to quinolines and its derivatives) [103]. Based on the catalyst preparative strategy, other types of material can be fabricated by anchoring various active species on N-doped hierarchical PCs. In another study, Yun *et al.* [104] reported the hydrogenation of quinolines **2** using a nitrogen-rich PC-stabilized Ni-Co NPs catalyst. Nitrogen-rich PC stabilized Ni-Co bimetallic nanoparticles developed by calcination of Ni-ZIF@ZIF-67 under an argon atmosphere and estimated its catalytic activity in chemo-selective hydrogenation of quinolines **2**. The synthesized catalyst exhibited excellent dispersion of Ni-Co NPs embedded in NC. This newly designed and developed selective and reusable catalyst could be used for the hydrogenation of heterocycles.

Biomass-derived N-doped porous two-dimensional carbon nanosheets (NPCNs) supported Ru catalyst developed by Cao *et al.* [105] and successfully employed in the selective hydrogenation of quinolines **2** under mild conditions (Fig. 7). NPCNs were prepared using biomass (glucose) as a carbon source and carbon nitride (g-C_3N_4) as both a template and a nitrogen source. The catalyst was characterized by various analytical methods. The XRD analysis revealed the existence of graphite planes, TEM image showed homogeneous distribution of Ru NPs throughout NPCNs with 1.66 nm size; while XPS analysis showed Ru^0 was the major phase on the

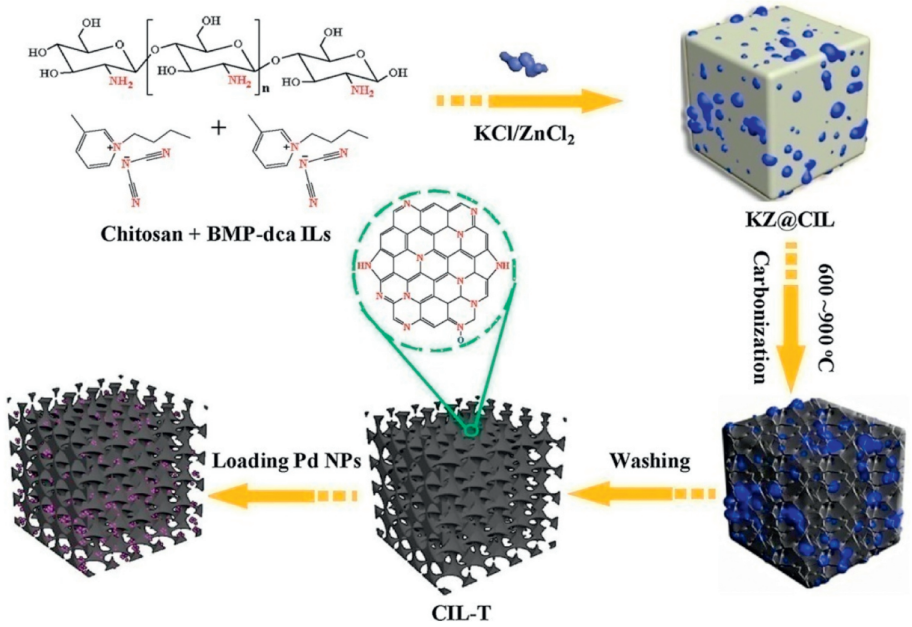

Scheme 17. The preparation procedure of Pd@CIL-T ($T = 600–900$ °C) catalyst. Reproduced with permission [102]. Copyright 2018, Elsevier.

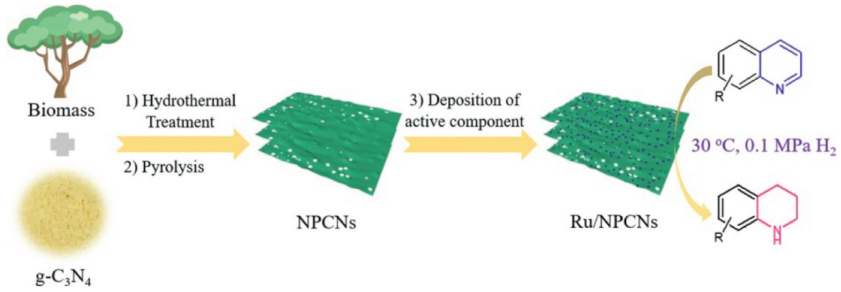

Fig. 7. Ru/NPCNs catalyst preparation and catalytic applications. Reproduced with permission [105], Copyright 2020, Elsevier.

surface of the catalyst. These analytical results demonstrate the formation of the catalyst. This NPCNs-supported Ru catalyst played a significant role in the hydrogenation of quinolines in ethanol at 30 °C with 98.1% to 99.5% conversion and up to 99.5% selectivity. The reusability test of the Ru/NPCNs catalyst revealed that, with its high stability, both the conversion and selectivity were almost preserved during at least up to the 5th run.

Kar and Srivastava [106] synthesized a cobalt-embedded porous N-doped PC catalyst and successfully employed it for the selective reduction and reductive *N*-formylation of *N*-heterocyclic arenes using formic acid as a H_2 donor and/or formylating source. For the preparation of N-doped PC catalyst, melamine was used as a nitrogen-rich source and OPD (*o*-phenylenediamine) **53** as a carbon source. In the presence of melamine, OPD was polymerized over colloidal silica as a hard template for porosity generation, and Co ($CoCl_2$ precursor) was embedded into the N-doped PC network (Scheme 18). The authors prepared various PC-supported Co catalysts. Compared to other catalysts, Co@C–N_{800} exhibited excellent catalytic performance. The XRD method showed the formation of graphitic planes in catalysts, which was well-supported by Raman spectra. The N_2-sorption experiments demonstrated that Co@C–N_{800} with 439 m^2/g of surface area, 1.89 cm^3/g of pore volume, and 6.9 nm pore diameter, while XPS analysis ascribed the higher concentration of C=C, and different species of Co NPs present in the catalysts. A sheet-like morphology and Co NPs embedded in catalysts were shown by TEM images (Fig. 8) while the

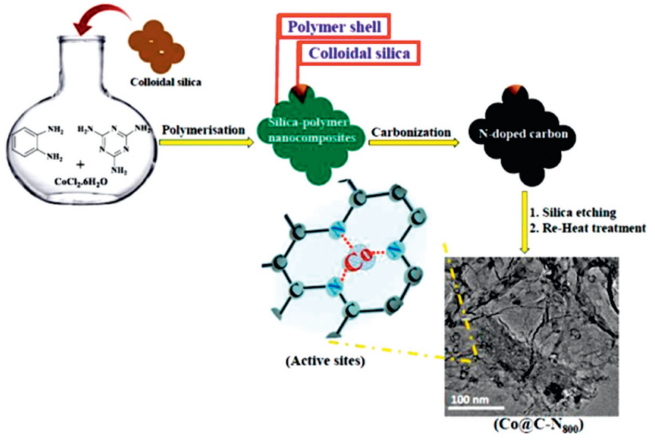

Scheme 18. Step-wise preparation of Co@C–N_x materials. Reproduced with permission [106]. Copyright 2019, American Chemical Society.

HAADF image and elemental maps clearly demonstrated the homogeneous dispersion of Co species in the catalysts.

Co@C–N_{800} catalyst was employed for the selective reduction of quinoline derivatives in the water at 130 °C that offered up to 85.6% yield. Moreover, Co@C–N_{800} exclusively catalyzed the formation of *N*-formyltetrahydroquinoline (FTHQ) **63** in toluene at 140 °C

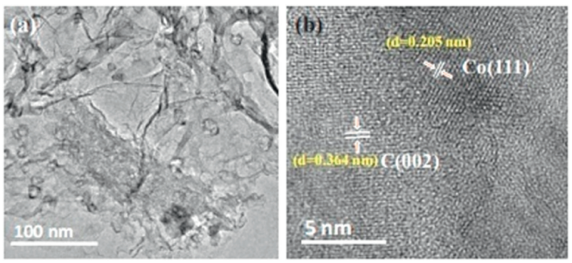

Fig. 8. (a) TEM image and (b) HR-TEM image of Co@C–N_{800} catalyst. Reproduced with permission [106]. Copyright 2019, American Chemical Society.

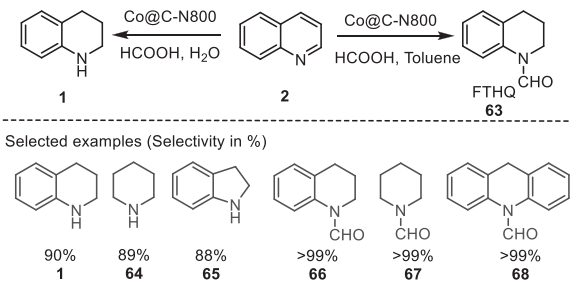

Scheme 19. Synthesis of THQ and FTHQ using Co@C–N_{800} catalyst.

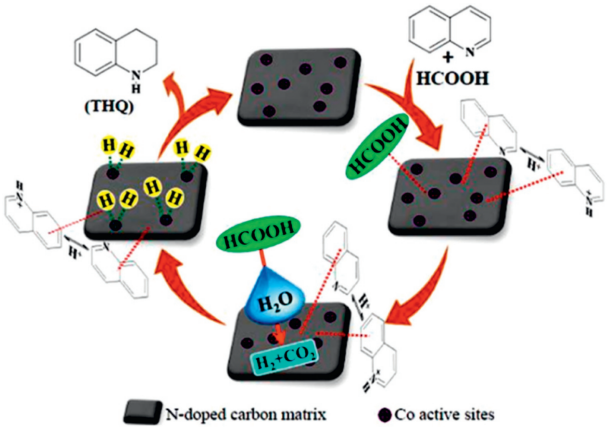

Scheme 20. A plausible mechanism for the catalytic transfer hydrogenation of quinoline in aqueous medium. Reproduced with permission [106]. Copyright 2019, American Chemical Society.

with 98% yield (Scheme 19). Striking aspects of this method include the implication of inexpensive transition metal-based catalyst, catalytic reusability, a wide scope of catalyst in heterocyclization, operation simplicity, and good to the excellent yield of the product.

The structure-activity relationship was established using quinoline **2** adsorption, CO_2-temperature program desorption, control reactions, and various spectral measurements. Catalytic reusability was tested for five consecutive cycles that showed a negligible catalytic loss. A simple catalyst synthesis procedure, its high-yielding ability, and recyclability signify that the catalyst could be used in industrial processes at the commercial level. A mechanistic study showed that *in-situ* generation of H_2 from HCOOH adsorbed on the catalyst surface that was efficiently transferred to quinolines adsorbed on the neighboring sites resulting in the formation of THQ with a high yield (Scheme 20).

By using a liquid-free nanocasting method, Xu and co-workers [107] prepared nanostructured PCs with different pore geometries. In this method, instead of liquid, gases are used to disperse the carbon precursor, remove impurities, leach templates, reduce synthetic steps, and the use of chemicals. They have prepared 12 different PCs using ferrocene as a carbon source and various template sources. From the resulting material, two PC-supported Ru clusters were used for the hydrogenolysis of HMF **29** and electrochemical hydrogen evolution (HER). It was found that Ru on bottle-neck pore carbon showed excellent performance in the conversion of HMF **29** to DMF **69** with 75% yield and 98% selectivity (Scheme 21).

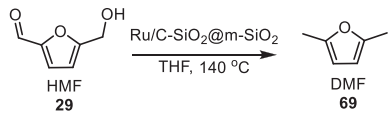

Scheme 21. Conversion of HMF to DMF using Ru/C-SiO_2@m-SiO_2 catalyst.

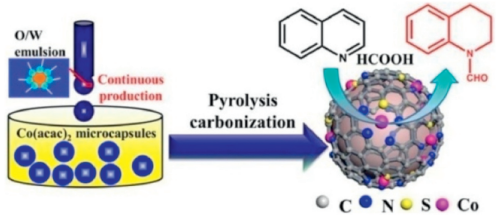

Scheme 22. *Quasi*-continuous synthesis of Co/SNC catalyst and its implication in the hydrogenation of quinoline. Reproduced with permission [116]. Copyright 2022, Elsevier.

Structure-activity relationship is established in HMF hydrogenolysis. The process of hydrogenolysis of 5-HMF comprises several steps. Initially, C=O is converted to C–OH, forming 2,5-hydroxymethylfuran (BHMF), then C–O cleavage is observed at the two hydroxyl groups, resulting in DMF **69**. The furan group can overreact with the H_2, forming *cis*- and *trans*-2,5-dimethyltetrahydrofuran (DMTHF). Another path to DMF is *via* the formation of 5-methylfurfural (5-MF).

The comparison in Table 3 [107–114] showed that using Ru/C-SiO_2@m-SiO_2 as a catalyst provides a higher yield of DMF at a low catalyst to 5-HMF molar ratio, at lower temperature, and in a shorter time.

A review of single-atom catalytic organic transformations has recently been reported by Hu *et al.* [115]. These catalytic systems showed remarkable activities to carry chemical reactions more efficiently. Similarly, PC-supported single-atom catalysts in heterocyclization reactions exhibited excellent performance. Hydrogenation of quinoline with formic acid using S,N co-doped carbon supported Co single-atom catalyst was achieved by Huang *et al.* [116]. The as-synthesized catalyst showed astonishing activity, selectivity, and reusability toward transfer hydrogenation of quinoline with 98% conversion and 99% selectivity (Scheme 22).

3.3. Isomerization/dehydration

Biomass-derived 5-hydroxymethylfurfural (HMF) **29** is a valuable platform chemical used in the food industry as a flavoring agent, in herbicides, plastic, solvents, in the metal-organic framework (MOF), in drugs, and widely recognized as a key intermediate in the fuel and polymer production [77]. The synthesis of **29** relies on Lewis base and Brønsted acid catalysis. It is a two-step mechanism involving the isomerization of glucose **70** to fructose **71** and further dehydration to HMF **29** [117]. Li *et al.* [118] have reported the efficient conversion of glucose **70** to 5-hydroxymethylfurfural (HMF) **29** using a hierarchical N-doped PC catalyst (SNC2–700) (Scheme 23). A series of catalysts such as SNC1–500, SNC1–600, SNC1–700, SNC1–800, SNC1–900, SNC2–700, SNC3–700, SC-700, and NC-700 were developed by polymerization, calcination, and

Table 3
Comparison of the catalytic result of Ru/C-SiO_2@m-SiO_2 with those in the literatures.

Catalyst	Reaction conditions					DMF yield (%)	Ref.
	Molar ratio (Cat./HMF)	Temp (°C)	Pressure (Bar)	Time (h)	Solvent		
Ru/C-SiO_2@m-SiO_2	0.035	140	10	2	THF	90	[107]
Cu/ZnO	0.657	220	15	1	1,4-Dioxane	41	[108]
Ru-NaY	0.005	220	15	1	THF	78	[109]
Ru/Co_3O_4	0.025	130	7	24	THF	93	[110]
PtCo@HGS	0.065	180	10	2	BuOH	98	[111]
Pd/C/$ZnCl_2$	0.12	150	8	8	THF	85	[112]
Raney Ni	0.72	180	15	15	1,4-Dioxane	88.5	[113]
Ru/C	Not indicated	180	15	2	THF	94.7	[114]

Scheme 23. Preparation of hierarchical porous N-doped carbon catalyst and its implication for HMF synthesis. Reproduced with permission [118]. Copyright 2021, American Chemical Society.

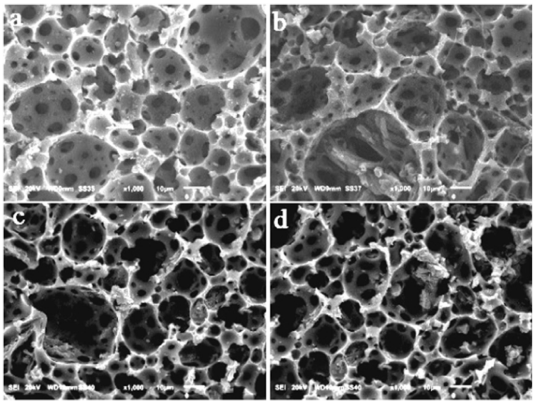

Fig. 9. SEM images of (a) SNC2–700, (b) SNC3–700, (c) NC-700, and (d) SC-700. Reproduced with permission [118]. Copyright 2021, American Chemical Society.

subsequent sulfonation under the Pickering technique. They have used styrene (divinylbenzene (DVB)) and 1-vinyl imidazole as carbon and nitrogen sources, respectively. The SEM images (Fig. 9) revealed that all samples have open pores and cross-linked pore structures, which were well protected from calcination and sulfonation processes. FTIR spectra of the catalyst showed that the N-doped carbon material was formed during the carbonization process and the presence of the -SO_3H group indicates success of the sulfonation step. The SNC2–700 catalyst with Brønsted acid and base sites exhibited remarkable activity in a one-pot synthesis of glucose **70** to HMF **29** with a yield of 61.3% and selectivity of 65.1%. A hierarchical porous N-doped carbon catalyst was successfully synthesized by the Pickering HIPE technique which has excellent thermal stability, high specific surface area, and acid-base bifunctional active sites. Furthermore, the catalytic activity was markedly enhanced due to the synergistic effect of acid-base sites. The catalyst also demonstrated excellent reusability, maintaining a high HMF **29** yield for up to four consecutive runs.

A plausible mechanism for converting glucose to HMF using a catalyst has been demonstrated by the authors (Scheme 24). The reaction of glucose was performed over an SNC2–700 catalyst having Brønsted acid and base sites. Initially, glucose was isomerized to fructose under the action of basic sites on the catalyst, while acid sites accelerate the dehydration of fructose to produce HMF **29**.

Although the SNC2–700 catalyst has acid-base bifunctional active sites, good thermal stability, and reusability, the present method offers moderate yield (61.3%), and selectivity (65.1%) of HMF **29** compared to the results presented in Table 4 [119–130]. By adjusting the Pickering HIPE parameters and nitrogen-doped contents, SNC catalysts can have their porous structure and basicity modified, which will help increase the yield of the HMF **29**.

3.4. Reaction

N–Heterocycles are an important class of organic compounds found in various natural products, biologically active structures, and medicinally relevant scaffolds. They are used as the building blocks of several new drug candidates due to the ability of nitrogen atoms to form H-bonding with biological targets. Among them, quinolines, quinazolines, quinazolinones, imidazoles, and indoles have gained considerable attention in medicinal chemistry, materials science, and organic synthesis. These compounds have a wide spectrum of biological and medicinal properties, like anticancer, antiviral, antibacterial, and many more [131].

Song and co-workers [132] reported the synthesis of *N*-heterocycles such as quinazolines **72**, imidazoles **76**, and quinazolinones **28**, *via* oxidative cross-dehydrogenative coupling of alcohols **73** and diamines **74**, or 2-aminobenzamides **75** using N,P-codoped biomass-derived PC as a catalyst, in the presence *t*BuOK, in toluene as a solvent, and air as the sole oxidant under milder reaction conditions (Scheme 25). In the catalyst preparation, bamboo shoots were used as a carbon source. Bamboo shoot biochar was mixed in an aqueous solution with $Ni(OAc)_2$ and phytic acid as Ni and P sources, respectively. Then, dry powder was calcined at 800 °C in the N_2 flow. The developed catalyst (Ni_2P@NPC-800) showed excellent catalytic activity in the synthesis of *N*-heterocycles.

Ni_2P@NPC-800 catalyst was characterized by various analytical techniques. TEM images (Fig. 10) showed uniform dispersion of Ni_2PNPs (3.2 ± 0.7 nm) on the graphitic carbon. EDX analysis exhibited homogeneous Ni, N, P, O, and C distribution throughout the carbon skeleton. The formation of Ni_2P@NPC-800 phase was indicated by the XRD method, while N_2 adsorption/desorption measurements explored that the catalyst possessed micro-, meso–, and macro-pores with large surface area and pore volume. The appear-

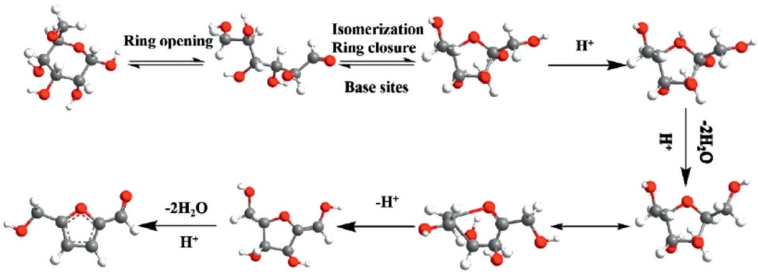

Scheme 24. The plausible mechanism for glucose to HMF conversion using acid-base bi-functional catalyst. Reproduced with permission [118]. Copyright 2021, American Chemical Society.

Table 4
Representative catalysts for the conversion of glucose to HMF.

Catalyst	Glucose conversion (%)	Time (h)	HMF yield (%)	Temp. (°C)	Solvent	Ref.
Al/Sn-HAP		3	70.5	130	EMIMBr	[119]
C_3N_4-supported UiO-66-type MOFs	92.0	6	54.9	120	Isopropanol/DMSO	[120]
Cr-β		1	58.5	130	BMIMCl	[121]
UiO-66-SO_3H–NH_2/PDA@PU		2	70.3	120	DMSO	[122]
Nb-β zeolite	97.4	12	82.1	180	Water/MIBK	[123]
Nb_4W_4	36.1	2	18.8	120	Water	[124]
γ-Al_2O_3	96	0.2	52	175	Water/MIBK	[125]
$Nb_{0.2}$-WO_3 + HCl	100	3	38	120	THF/water	[126]
Al-KCC-1 (Si/Al=5,40)	97.8	2	39	170	DMSO	[127]
Al_2O_3-b-0.05	91	3	49.7	140	EMIMBr	[128]
Fe_3O_4@SiO_2-SO_3H	98	24	70.5	140	Water/MIBK	[129]
TiO_2/Nb_2O_5•nH_2O	97	5	42	150	Water	[130]

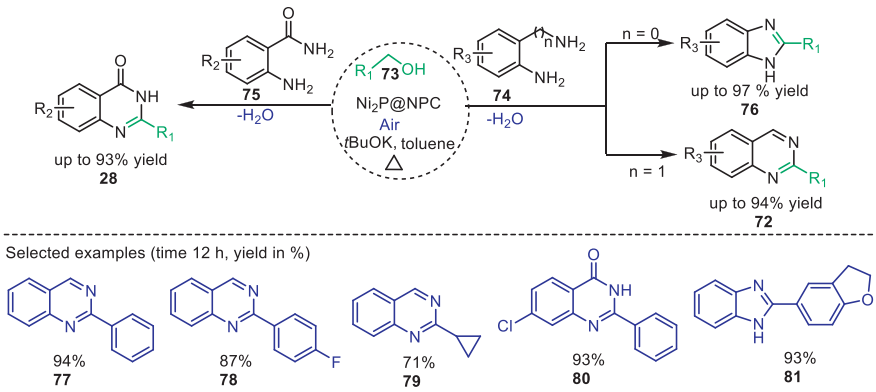

Scheme 25. Synthesis of *N*-heterocycles using Ni_2P@NPC catalyst.

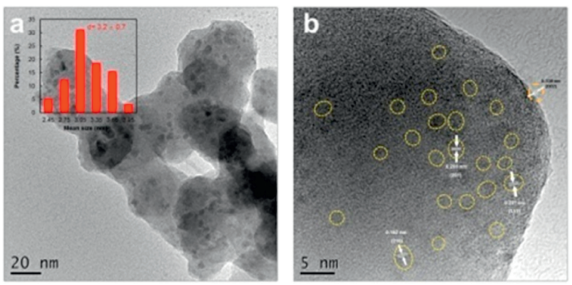

Fig. 10. (a) TEM and (b) HR-TEM images of Ni_2P@NPC-800 catalyst. Reproduced with permission [132]. Copyright 2020, American Chemical Society.

ance of nitrogen (in pyridinic, pyrrolic, graphitic, and oxidized) and the bond formation between C and P, N, and O have been well-demonstrated by XPS analysis. Ni_2P@NPC-800 catalyst with good functional group tolerance, high catalytic activity, abundant feedstock bamboo as a carbon source, broad substrate scope, mild reaction conditions, operation simplicity, and up to 97% yield of the desired products indicate the protocol to be practical for the synthesis of *N*-heterocycles.

In the case of quinazolines **72** and benzimidazoles **76** syntheses, aromatic alcohols **73** with electron donating groups exhibited higher reactivity, while aliphatic alcohols needed elevated temperatures to get high yields. The catalytic activity was also investigated for the synthesis of a novel cardiotonic vasodilator agent pimobendan **84**, which offered a 57% yield under the optimized reaction conditions (Scheme 26). The mechanism for the formation of *N*-heterocycles has been proposed *via* oxidative cross-dehydrogenative coupling of alcohols and diamines or 2-aminobenzamides (Scheme 27). The reaction proceeds through the following steps, in the first step, the oxidative dehydrogenation of alcohol to aldehyde to generate the [NiH] species in the presence of the base. In the second step, aldehyde and diamines or 2-aminobenzamides undergo condensation to form tetrahydrohydroquinazoline, dihydroquinazolin-4(1*H*)-one, or dihydrobenzoimidazole, and in the final step, oxidative dehydrogenative aromatization catalyzed by Ni_2P and the base to afford the *N*-heterocycles.

Because of their potent bioactivity, 2-benzofurans **87** have attracted considerable interest. Ji *et al.* [133] reported the synthe-

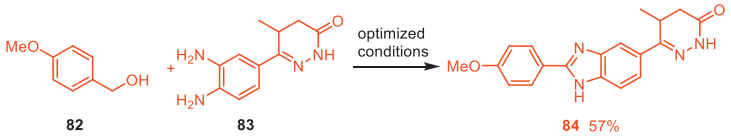

Scheme 26. Synthesis of pimobendan.

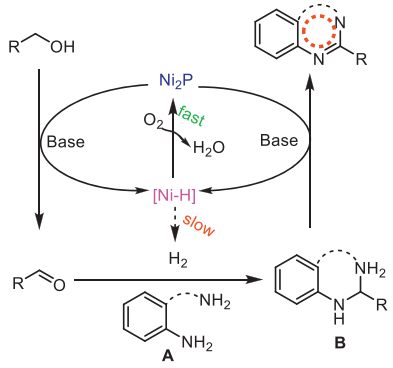

Scheme 27. Proposed mechanism for the synthesis of *N*-heterocycles.

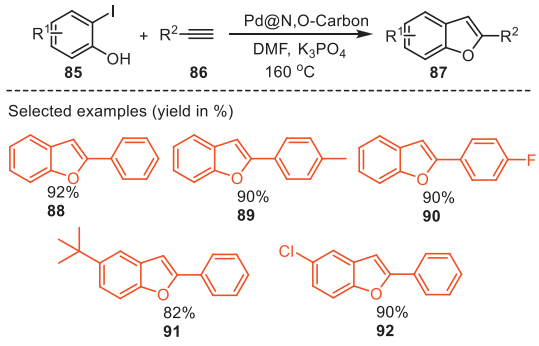

Scheme 28. Synthesis of 2-benzofuran derivatives.

sis of 2-benzofuran derivatives **87** *via* the Sonogashira/cyclization reaction of *o*-iodophenol **85** with terminal alkynes **86** using Pd/N,O–Carbon catalyst under ligand-/copper-free conditions (Scheme 28). The bamboo shoot was used as a natural source to create PC.

The catalyst was developed by hydrothermal treatment and carbonization process. Powdered bamboo shoots were added to the deionized water and heated at 180 °C in an autoclave. Then, the powder was carbonized at 850 °C in the N_2 flow. The developed catalyst was denoted as N,O–Carbon. Further, N,O–Carbon (0.15 g) was dispersed in the water (100 mL) under ultrasonic conditions for 30 min. then, an aqueous solution of $Pd(NO_3)_2$ (0.268 wt%) was added to it and stirred vigorously for 1 h. The pH of the solution was adjusted to 11 by adding an ammonia solution. Then, by adding hydrazine (0.2 mL), the mixture was heated at 80 °C in an oil bath. The resulting product was filtered, washed with deionized water, and dried. The obtained Pd/N,O–Carbon was used as a catalyst for the synthesis of 2-benzofurans in the DMF solvent, in the presence of K_3PO_4 at 160 °C under an argon atmosphere that offered up to 92% yield. Catalytic recycling experiments have shown a negligible change in the activity and selectivity after the 5th run.

Quinoxaline **94** is an important class of heterocyclic motif, showing a wide variety of biological activities such as anti-viral, antibacterial, anti-cancer, and neurological activity; it also inhibits metal corrosion [134]. The coupling between 1,2-diketones or 2-aminobenzyl alcohol and 1,2-diamines for the synthesis of

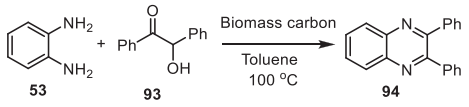

Scheme 29. Porous carbon catalyzed synthesis of quinoxalines.

quinoxalines has been well documented in literature [135]. Perez-Mayoral *et al.* [136] reported acid biomass-derived PC with high BET surface area and pore volume that efficiently catalyzed quinoxaline **94** synthesis under aerobic conditions. The stalks of the invasive plant *Hedychium gardnerianum* were used as carbon feedstock. The authors prepared three carbon series with different porous structures, such as plant-derived carbons activated by H_3PO_4, xerogel mesoporous carbon from resorcinol-formaldehyde polymerization, and ordered mesoporous carbon from phenol. Catalytic characterization was performed using different techniques. N_2-sorption showed BET surface area (2197 m^2/g), and pore volume (1.39 cm^3/g) with wider micropores. The presence of P and high O content was confirmed by XPS studies. FTIR spectra exhibited the presence of P and O bonded with the carbon skeleton, while Raman spectra showed a disordered carbon structure. The prepared catalysts were tested in the synthesis of quinoxaline **94** from *o*-phenylenediamine **53** and benzoin **93** under aerobic conditions in toluene at 100 °C (Scheme 29). Notably, biomass-derived PCs revealed high activity in the quinoxaline **94** synthesis, with 94% conversion and 83% selectivity. Additionally, dihydropyrazine was synthesized from ethylenediamine and benzoin **93** under similar reaction conditions with 96% yield and 96% selectivity. This method yields quantitatively, but examining the effect of solvent, temperature, and other reaction conditions on yield and efficiency would have been useful in diverse organic transformations.

3.5. CO_2 fixation

Greenhouse gas CO_2 has been considered one of the main sources of environmental pollution. Diversion of CO_2 in the synthesis of organic compounds would be economically and environmentally benign due to the non-toxicity, abundance, non-flammability, and renewable features of CO_2. A C_1 feedstock, carbon dioxide undergoes cycloaddition with epoxides yielding organic cyclic carbonates, a functionality possessing significant industrial applications [137]. Polidoro and co-workers [138] have used CO_2 for the synthesis of organic cyclic carbonates **57** on metal-free N-doped carbon catalysts derived from chitosan, chitin, and shrimp shell waste. Catalytic materials were well-characterized by various analytical methods. CNHS analysis indicated that the N-content was 10% ± 1%, and 6% ± 1% for C4–500 and C5–500 catalysts, respectively. N_2-sorption demonstrated that the C4–500 catalyst has a surface area of 321 m^2/g, pore volume of 0.38 cm^3/g, and pore diameter of 4.5 nm, while C5–500 has a surface area of 7 m^2/g, pore volume of 0.05 cm^3/g, and pore diameter of 26.8 nm. SEM images indicated that the catalysts were composed of C, N, and O along with Ca, P, and S. The XPS analysis showed the presence of C, N, and O as well as pyridinic and pyrrolic species.

Carbonized chitin catalyst under batch conditions showed excellent activity in the conversion of epoxide derivatives **95** into

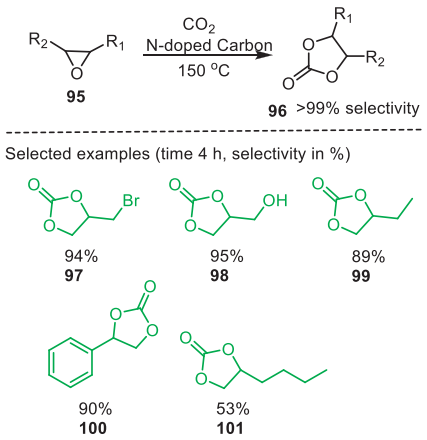

Scheme 30. Synthesis of cyclic carbonates over N-doped carbon catalyst.

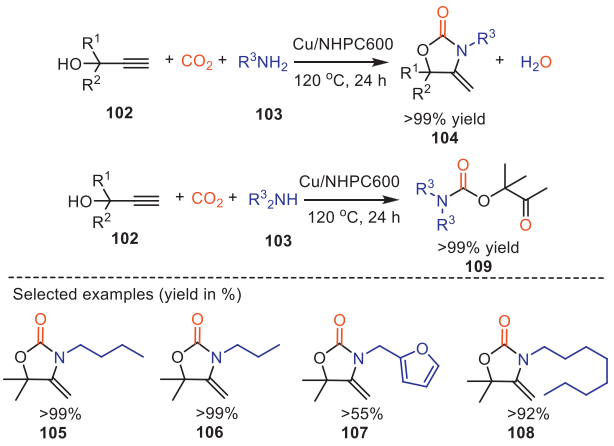

Scheme 31. Cu/NHPC promoted chemical fixation of CO_2 to oxazolidinone and β-oxopropylcarbamates.

cyclic carbonates **96** at 150 °C and 30 bar CO_2 for 4 h with 96% selectivity. While under a continuous flow regime, carbonate selectivity was >99% at 150 °C using a shrimp waste-derived catalyst (Scheme 30). The as-developed catalysts exhibited excellent performance with operational stability and reusability. Catalytic activity may be associated with more basic pyridinic sites.

Oxazolidinones **104** and β-oxoalkyl carbamates **109** are biologically active compounds used in agriculture as herbicides, fungicides, medical raw materials, and synthetic intermediates [139,140]. Because of the potent bioactivity of **104** and **109**, Chen and co-workers [141] reported the synthesis of these compounds using transition-metal complexes as heterogeneous catalysts. They demonstrated that heterogeneous catalysts of highly dispersed Cu supported on hierarchically porous N-doped carbon (NHPC) could efficiently promote CO_2 fixations to **104** and **109** (Scheme 31). NHPC catalyst was developed by pyrolysis of nitrogen-containing polymer gel (NPG) in the presence of a $KHCO_3$ activator. The resulting NHPC exhibited a high surface area (2054 m^2/g) with average micro/meso/macropore size (0.55/3.2/50 nm to 230 nm), SEM micrograph (Fig. 11) showed the presence of macropores, while TEM exhibited a high dispersion of Cu species in the catalyst. Copper-supported NHPC catalyst was able to promote the three-component coupling of propargyl alcohols **102**, amines **103**, and CO_2 more efficiently to produce oxazolidiones **104**, and β-oxopropylcarbamates **109** with up to 99% yield. The catalyst also showed excellent recyclability up to the 9th run. This protocol therefore enhances green credentials.

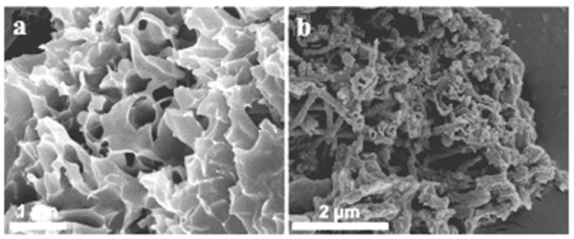

Fig. 11. SEM images of (a) NHPC and (b) Cu/NMC_{600} catalysts. Reproduced with permission [141]. Copyright 2020, American Chemical Society.

4. Conclusion and outlook

In this article, the state-of-the-art knowledge in the field of heterogeneous PC materials as catalysts and their endless applications in the synthesis of diverse and densely functionalized heterocyclic compounds have been reviewed. Potential heterogeneous catalysts, a high-tech material and a major contributor to industrial catalysis, typically possess active sites capable of providing a space for reactants to react and convert into products. In this concern, the PC material is a cheaper alternative to stoichiometric reagents, and traditional catalysts with fascinating properties including hierarchical porosity, high surface area, electron conductivity, and functionality. Because of these outstanding properties, PC can provide an active surface to carry out several pharmacologically important heterocyclic reactions with a quantitative yield of the desired products.

From the perspective of green chemistry, instead of expensive PGM group metals, the use of earth-abundant transition metals such as Fe, Ni, Cu, Zn, Mn, with PC support is highly desirable because of their low cost, easy availability, and environmental friendliness. Moreover, single-atom-doped PC (SAC) catalysts demonstrate excellent atom utilization efficiency, remarkable turnover frequency, and selectivity [10]. A few heterocyclic reactions have been reported using PC-based transition metals and SAC catalysts. Still, immense scope lies in designing and developing PC-based transition metals and SAC catalysts using earth-abundant transition metals and employing them in the synthesis of highly functional heterocycles. Commensurate with metal oxide-based catalysts, heterogeneous PC-based catalysts have unique properties, such as acidity, basicity, redox futures (electron transfer), electron conductivity, thermal conductivity effects, and giant π structures [142]. These properties facilitate strong interactions with various reactants, making PC-based catalysts a promising alternative to metal oxide-based catalysts.

Undoubtedly, purified organic compound is a potential source for PC creation. However, due to fossil fuel consumption, this carbon source is not economically feasible and environmentally benign. In contrast, low-cost, non-toxic, and readily available waste biomass is the best option for the PC's creation. However, biomass is composed of lignocellulosic components consisting of a polyhydroxy structure that leads to irregular and weak adsorption of metals, resulting in uneven and unstable metal species after pyrolysis. Therefore, efforts should be taken to improve the dispersibility and stability of metals. MOF and COF-derived PC materials exhibit high porosity, ultrahigh surface area, and abundant metal/organic species, resulting in excellent catalytic performance compared to conventional porous carbons. These studies provide an opportunity to develop highly active PC materials using MOFs or COFs.

Doping with N, S, or P can enhance the catalytic activity of PC. N-Doped PCs have three kinds of carbon bonds that are graphite sp^2 C, N-sp^2 C, and C=O bonds, while, in P-doped PCs, P is bonded with C (P-C) and or with O (P-O). As compared to PCs, P-doped PCs show excellent catalytic performance in heterocycles synthesis.

It is because P-doped PCs are electron-rich, with P atoms having lower electronegativity (2.19) than C (2.55) making P partially positively charged. Moreover, since the diameter of P is much larger than that of C, P-doping leads to more local structural distortion of the hexagonal carbon framework, and in such a configuration, P tends to be out of the graphene plane. Distinct effects by P-doping may also arise from the additional vacant 3d orbitals and the valence electrons in the third shell. All these characteristics empower P-doped carbon materials as proactive catalytic species. For the P-doped PC, instead of synthetic phosphorous sources, the use of natural phosphorus sources such as bird guano, bone meal, crab, and shrimp waste could increase the green credentials of the protocols.

PC-supported Brønsted acids and Lewis acids have a good scope in acid-catalyzed heterocyclization [143]; however, leaching of the sulfonic group from the catalytic surface leads to reduce the catalytic activity. Thus, efforts need to be taken for catalytic recovery and reusability of the sulfonic group-bearing PC material. Although Heteropoly acid (HPA) catalyst has high Brønsted acidity and tunable catalytic properties, one of the disadvantages of HPA catalyst is that its surface area is very low (<10 m^2/g). Heteropolyanions have a negative charge. If PC materials are modified to have a positive charge, they can support HPA and help increase surface area and catalytic activity.

In addition to oxidation, reduction, dehydrogenation, and cross-coupling, other reactions such as cycloaddition (*e.g.*, Aza Diels-Alder reaction), halogenations, Michel addition, Knoevenagel condensation, nitration, photocatalytic heterocyclization and many others can be performed using advanced PC materials. PC-based photocatalytic heterocyclization is also the subject of interest. The implications of PCs as support for photocatalysts are highly favorable. PC materials have good electrical conductivity, tunable photocatalytic activity in the visible light region, and scavenge photogenerated electrons from the photocatalyst surface. Additionally, due to the high surface area, the carbon material also increases the dispersion of photocatalysts and promotes CO_2 adsorption, resulting in enhanced photocatalytic reactions.

To conclude, the design and development of a new PC generation with sufficient and appealing physicochemical and textural properties to enable more sustainable heterocyclic synthesis with high synthetic yields and environmental standards is a challenging topic for future research.

Declaration of competing interest

The authors declare that they have no known competing financialinterestsor personal relationships that could have appeared to influence the work reported in this paper.

Acknowledgment

The author is thankful to ACS College, Palus, and Shivaji University, Kolhapur.

References

[1] U.P. Patil, S.S. Patil, Top. Curr. Chem. 379 (2021) 36.
[2] J. Hagen, Industrial Catalysis: A Practical Approach, 3ed, Wiley-VCH, Weinheim, 2015.
[3] Y. Cao, S. Mao, M. Li, Y. Chen, Y. Wang, ACS Catal. 7 (2017) 8090–8112.
[4] H.O. Pierson, Element Carbon, Noyes Publications Park Ridge, New Jersey, 1993.
[5] M. Inagaki, H. Itoi, F. Kang, Porous Carbons Synthesis and Applications, Elsevier Inc., 2022.
[6] M.N. Sarvi, T.B. Bee, C.K. Gooi, et al., Chem. Eng. J. 235 (2014) 244–251.
[7] L. Xu, L. Guo, G. Hu, et al., RSC Adv. 5 (2015) 37964–37969.
[8] J. Jampilek, Molecules 24 (2019) 3839.
[9] S. Chaudhuri, A. Ghosh, S.K. Chattopadhyay, Green Synthetic Approaches For Medium Ring-Sized Heterocycles of Biological and Pharmaceutical Interest, Elsevier, 2021.
[10] M. Li, F. Xu, H. Li, Y. Wang, Catal. Sci. Technol. 6 (2016) 3670–3693.
[11] Y. Lin, J. Yu, X. Zhang, et al., Chin. Chem. Lett. 33 (2022) 186–196.
[12] S. De, A.M. Balu, J.C. van der Waal, R. Luque, ChemCatChem 7 (2015) 1608–1629.
[13] A. Rai, K.V.S. Ranganath, J. Hetero. Chem. 58 (2020) 1039–1057.
[14] E. Pérez-Mayoral, I. Matos, M. Bernardo, I.M. Fonseca, Catalysts 9 (2019) 133.
[15] A. Khan, M. Goepel, J.C. Colmenares, R. Gläser, ACS Sustain. Chem. Eng. 8 (2020) 4708–4727.
[16] Y. Rangraz, M.M. Heravi, A. Elhampour, Chem. Rec. 21 (2021) 1985–2073.
[17] H. Li, L. Chen, X. Li, D. Sun, H. Zhang, Nano-Micro Lett. 14 (2022) 1–35.
[18] C. Xu, M. Stromme, Nanomater 16 (2019) 103.
[19] Y. Liang, C. Yang, H. Dong, et al., ACS Sustain. Chem. Eng. 5 (2017) 7111–7117.
[20] J. Mi, X.R. Wang, R.J. Fan, W.H. Qu, W.C. Li, Energy Fuels 26 (2012) 5321–5329.
[21] W. Lv, J. Xiang, F. Wen, et al., Electrochim. Acta 153 (2015) 49–54.
[22] C. Ma, J. Bai, M. Demir, et al., Sep. Purif. Technol. 303 (2022) 122299.
[23] N. Zhang, Y. Shen, Bioresour. Technol. 284 (2019) 325–332.
[24] S. Khedr, M. Shouman, N. Fathy, A. Attia, Int. Scholar. Res. Notices (2014) 1–10.
[25] J. Yin, W. Zhang, N.A. Alhebshi, N. Salah, H.N. Alshareef, Small Methods 4 (2020) 1900853.
[26] R.C. Bansal, J.B. Donnet, F. Stoeckli, Active Carbon, New York, 1988.
[27] H. Yi, K. Nakabayashi, S.H. Yoon, J. Miyawaki, Carbon 183 (2021) 735–742.
[28] A. Colomba, F. Berruti, C. Briens, J. Anal. Appl. Pyrolysis 168 (2022) 105769.
[29] J. Pallarés, A. González-Cencerrado, I. Arauzo, Biomass Bioenergy 115 (2018) 64–73.
[30] M.A.A. Zaini, L.L. Zhi, T.S. Hui, Y. Amano, M. Machida, Mater. Today: Proc. 39 (2021) 917–921.
[31] M. Gao, S.Y. Pan, W.C. Chen, P.C. Chiang, Mater. Today Energy 7 (2018) 58–79.
[32] Z. Heidarinejad, M.H. Dehghani, M. Heidari, et al., Environ. Chem. Lett. 18 (2020) 393–415.
[33] Z. Pan, S. Yu, L. Wang, et al., Nanomaterials 13 (2023) 1744.
[34] P.J. Johnson, D.J. Setsuda, R.S. Williams, Activated carbon for automotive applications, in: T.D. Burchell (Ed.), Carbon Materials for Advanced Technologies, Elsevier Science Ltd., 1999, pp. 235–268.
[35] M.K.B. Gratuito, T. Panyathanmaporn, R.A. Chumnanklang, N. Sirinuntawittaya, A. Dutta, Bioresour. Technol. 99 (2008) 4887–4895.
[36] X. Cui, F. Jia, Y. Chen, J. Gan, Ecotoxicology 20 (2011) 1277–1285.
[37] N. Wang, T. Li, Y. Song, J. Liu, F. Wang, Carbon 130 (2018) 692–700.
[38] J. Jjagwe, P.W. Olupot, E. Menya, H.M. Kalibbala, J. Bioresour. Bioprod. 6 (2021) 292–322.
[39] K. Adlak, R. Chandra, V.K. Vijay, K.K. Pant, J. Anal. Appl. Pyrolysis 155 (2021) 105102.
[40] W. Ao, J. Fu, X. Mao, et al., Renew. Sustain. Energy Rev. 92 (2018) 958–979.
[41] Y. Gao, Q. Wang, G. Ji, A. Li, J. Niu, RSC Adv. 11 (2021) 5361–5383.
[42] B. Wang, T.P. Ang, A. Borgna, Microporous Mesoporous Mater. 158 (2012) 99–107.
[43] S. Zhang, X. Zhang, S. Zhang, et al., Carbon Capture Sci. Technol. 9 (2023) 100135.
[44] Z. Wang, K.G. Burra, T. Lei, A.K. Gupta, Prog. Energy Combust. Sci. 84 (2021) 100899.
[45] Y. Xu, R.S. Sprick, N.J. Brownbill, et al., J. Mater. Chem. A 9 (2021) 3303–3308.
[46] H. Li, X. Fang, F. Lv, et al., Nano Res. 16 (2023) 3879–3887.
[47] R. Wang, R. Wu, X. Yan, et al., Adv. Funct. Mater. 32 (2022) 2200424.
[48] L. Jiao, G. Wan, R. Zhang, et al., Angew. Chem. Int. Ed. 57 (2018) 8525.
[49] T. Kyotani, Carbon 38 (2000) 269–286.
[50] S. Mehdipour-Ataei, E. Aram, Catalysts 13 (2023) 2.
[51] W. Xin, Y. Song, RSC Adv. 5 (2015) 83239–83285.
[52] F. Schüth, Angew. Chem. Int. Ed. 42 (2003) 3604–3622.
[53] N. Díez, M. Sevilla, A.B. Fuertes, Carbon 178 (2021) 451–476.
[54] W. Zhang, R. Cheng, H. Bi, et al., New Carbon Mater. 36 (2021) 69–81.
[55] C.X. Bai, F. Shen, X.H. Qi, Chin. Chem. Lett. 28 (2017) 960–962.
[56] L. Xie, Z. Jin, Z. Dai, et al., Carbon 170 (2020) 100–118.
[57] N. Mei, Z. Lei, L. Yancen, N. Runtao, Front. Chem. 11 (2023) 1–5.
[58] Q. Wang, Y. Mu, W. Zhang, et al., RSC Adv. 4 (2014) 32113–32116.
[59] Y. Hu, C. Tang, H. Li, et al., Chin. Chem. Lett. 33 (2022) 480–485.
[60] A.G. Sadekar, S.S. Mahadik, A.N. Bang, et al., Chem. Mater. 24 (2012) 26–47.
[61] X. Yang, D. Yang, G. Zhang, H. Zuo, J. Power Sources 482 (2021) 229135.
[62] C. Liang, Z. Li, S. Dai, Angew. Chem. Int. Ed. 47 (2008) 3696–3717.
[63] U.P. Patil, R.C. Patil, S.S. Patil, J. Hetero. Chem. 56 (2019) 1898–1913.
[64] U.P. Patil, R.C. Patil, S.S. Patil, Reac. Kinet. Mech. Cat. 129 (2020) 679–691.
[65] U.P. Patil, R.C. Patil, S.S. Patil, Org. Prep. Proced. Int. 53 (2021) 190–199.
[66] X. Wang, Z. Wang, Z. Li, K. Sun, Chin. Chem. Lett. 34 (2023) 108045.
[67] C. Tran, A. Abdallah, V. Duchemann, G. Lefèvre, A. Hamze, Chin. Chem. Lett. 34 (2023) 107758.
[68] R.I. Kureshy, I. Ahmad, K. Pathak, et al., Catal. Commun. 10 (2009) 572–575.
[69] L. Han, Z. Yuan, X. Shao, X. Xu, Z. Li, Chin. Chem. Lett. 34 (2023) 107868.
[70] U.P. Patil, S.U. Patil, Indian J. Chem. Technol. 30 (2023) 265–277.
[71] M.K. Sahoo, E. Balaraman, Green Chem. 21 (2019) 2119–2128.
[72] K. Sun, H. Shan, R. Ma, et al., Chem. Sci. 13 (2022) 6865.
[73] M. Krivec, M. Gazvoda, K. Kranjc, et al., J. Org. Chem. 77 (2012) 2857–2864.
[74] T. Su, K. Sun, G. Lu, C. Cai, ACS Sustain. Chem. Eng. 10 (2022) 3872–3881.
[75] J.J. Liu, F.H. Guo, F.J. Cui, et al., New J. Chem. 46 (2022) 1791–1799.
[76] C. Yang, X. Li, Z. Zhang, et al., Fuel 278 (2020) 118361.
[77] F.A. Kucherov, L.V. Romashov, K.I. Galkin, et al., ACS Sustain. Chem. Eng. 6 (2018) 8064–8092.
[78] J.P. Ma, Z.T. Du, J. Xu, Q.H. Chu, Y. Pang, ChemSusChem 4 (2011) 51–54.

[79] Q. Girka, N. Hausser, B. Estrine, et al., Green Chem. 19 (2017) 4074–4079.
[80] R. Fang, R. Luque, Y. Li, Green Chem. 18 (2016) 3152–3157.
[81] A. Corma, O. de la Torre, M. Renz, ChemSusChem 4 (2011) 1574–1577.
[82] J. Artz, S. Mallmann, R. Palkovits, ChemSusChem 8 (2015) 672–679.
[83] Z.H. Zhang, Z.L. Yuan, D.G. Tang, et al., ChemSusChem 7 (2014) 3496–3504.
[84] A. Takagaki, M. Takahashi, S. Nishimura, K. Ebitani, ACS Catal. 1 (2011) 1562–1565.
[85] C. Po-Yee, B. Zhao-Xiang, P. Ho-Yuen, et al., Future Med. Chem. 7 (2015) 947–967.
[86] J. Marco-Contelles, E. Prez-Mayoral, A. Samadi, et al., Chem. Rev. 109 (2009) 2652–2671.
[87] M. Godino-Ojer, S. Morales-Torres, E. Prez-Mayoral, et al., J. Environ. Chem. Eng. 10 (2022) 106879.
[88] J. López-Sanz, E. Pérez-Mayoral, E. Soriano, et al., ChemCatChem 5 (2013) 3736–3742.
[89] Z. Chen, J. Song, X. Peng, S. Xi, et al., Adv. Mater. 33 (2021) 2101382.
[90] A. Corma, O. de la Torre, M. Renz, et al., Energ. Environ. Sci. 5 (2012) 6328–6344.
[91] R. Zhong, Y. Liao, B.F. Sels, et al., ACS Sustain. Chem. Eng. 6 (2018) 7859–7870.
[92] I.F. Florentino, D.P.B. Silva, D.M. Silva, et al., Nitric Oxide 69 (2017) 35–44.
[93] Y. Yoon, B.R. Kim, C.Y. Lee, J. Kim, Asian J. Org. Chem. 5 (2016) 746–749.
[94] P. Zhang, E.A. Terefenko, et al., J. Med. Chem. 45 (2002) 4379–4382.
[95] X. Long, J. Wang, G. Gao, et al., ACS Catal. 11 (2021) 10902–10912.
[96] R.K. Singh, S. Sharma, A. Kaur, M. Saini, S. Kumar, Iran. J. Catal. 6 (2016) 1–22.
[97] S. Grattini, E. Mussini, L.O. Randall, Benzodiazepines, Raven Press, New York, 1973, p. 27.
[98] M. Godino-Ojer, I. Matos, E. Perez-Mayoral, et al., Catal. Today 357 (2020) 64–73.
[99] I. Muthukrishnan, V. Sridharan, J.C. Menendez, Chem. Rev. 119 (2019) 5057–5519.
[100] Y. Gong, P. Zhang, X. Xu, et al., J. Catal. 297 (2013) 272–280.
[101] X. Wang, W. Chen, L. Zhang, et al., J. Am. Chem. Soc. 139 (2017) 9419–9422.
[102] F. Zhang, C. Ma, S. Chen, et al., Mole. Catal. 452 (2018) 145–153.
[103] D. Ren, L. He, L. Yu, et al., J. Am. Chem. Soc. 134 (2012) 17592–17598.
[104] R. Yun, L. Hong, W. Ma, S. Wang, B. Zheng, ACS Appl. Nano Mater. 2 (2019) 6763–6768.
[105] Y. Cao, L. Ding, Z. Qiu, H. Zhang, Catal. Commun. 143 (2020) 106048.
[106] A.K. Kar, R. Srivastava, ACS Sustain. Chem. Eng. 7 (2019) 13136–13147.
[107] R. Xu, L. Kang, J. Knossalla, et al., ACS Nano 13 (2019) 2463–2472.
[108] Y. Zhu, X. Kong, H. Zheng, et al., Catal. Sci. Technol. 5 (2015) 4208–4217.
[109] A.S. Nagpure, N. Lucas, S.V. Chilukuri, ACS Sustain. Chem. Eng. 3 (2015) 2909–2916.
[110] Y. Zu, P. Yang, J. Wang, et al., ACS Sustain. Chem. Eng. 146 (2014) 244–248.
[111] G.H. Wang, J. Hilgert, F.H. Richter, et al., Nat. Mater. 13 (2014) 293.
[112] B. Saha, C.M. Bohn, M.M. Abu-Omar, ChemSusChem 7 (2014) 3095–3101.
[113] X. Kong, Y. Zhu, H. Zheng, et al., RSC Adv. 4 (2014) 60467–60472.
[114] L. Hu, X. Tang, J. Xu, et al., Ind. Eng. Chem. Res. 53 (2014) 3056–3064.
[115] H. Hu, J. Xi, Chin. Chem. Lett. 34 (2023) 107959.
[116] L. Huang, H. Zhang, Y. Cheng, et al., Chin. Chem. Lett. 33 (2022) 2569–2572.
[117] S. Zhong, R. Daniel, H. Xu, et al., Energy Fuels 24 (2010) 2891–2899.
[118] B. Li, Y. Chen, W. Guan, et al., Energy Fuels 35 (2021) 4191–4202.
[119] Y. Nie, Q. Hou, C. Bai, et al., J. Cleaner Prod. 274 (2020) 123023.
[120] Y.L. Zhang, W. Guan, H. Song, et al., Microporous Mesoporous Mater. 305 (2020) 110328.
[121] E. Sezgin, M.E. Kececi, S. Akmaz, S.N. Koc, Cellulose 26 (2019) 9035–9043.
[122] Y.L. Zhang, J.J. Zhao, K. Wang, et al., ChemistrySelect 3 (2018) 9378–9387.
[123] N. Candu, M.E. Fergani, M. Verziu, et al., Catal. Today 325 (2019) 109–116.
[124] J. Guo, S. Zhu, Y. Cen, et al., Appl. Catal. B 200 (2017) 611–619.
[125] C. García-Sancho, I. Fúnez-Núñez, R. Moreno-Tost, et al., Appl. Catal. B: Environ. 206 (2017) 617–625.
[126] C. Yue, G. Li, E.A. Pidko, et al., ChemSusChem 9 (2016) 2421–2429.
[127] F. Shahangi, A.N. Chermahini, M.J.J. Saraji, J. Energy Chem. 27 (2018) 769–780.
[128] Q.D. Hou, M.N. Zhen, W.Z. Li, et al., Appl. Catal. B 253 (2019) 1–10.
[129] I. Elsayed, M. Mashaly, F. Eltaweel, M.A. Jackson, E.B. Hassan, Fuel 221 (2018) 407–416.
[130] F.M. Huang, T.Y. Jiang, X.C. Xu, et al., P.J. Catal. Sci. Technol. 10 (2020) 7857–7864.
[131] B. Zhang, A. Studer, Chem. Soc. Rev. 44 (2015) 3505–3521.
[132] T. Song, P. Ren, Z. Ma, J. Xiaoc, Y. Yang, ACS Sustain. Chem. Eng. 8 (2020) 267–277.
[133] G. Ji, Y. Duan, S. Zhang, Y. Yang, Catal. Today 330 (2019) 101–108.
[134] J.A. Pereira, A.M. Pessoa, et al., Eur. J. Med. Chem. 97 (2015) 664–672.
[135] S. Shee, D. Panja, S. Kundu, J. Org. Chem. 85 (2020) 2775–2784.
[136] M. Godino-Ojer, R. Blazquez-García, E. Perez-Mayoral, et al., Catal. Today 354 (2020) 90–99.
[137] M.H. Beyzavi, C.J. Stephenson, et al., Front. Energy Res. 2 (2015) 128097.
[138] D. Polidoro, A. Perosa, E. Rodriquez-Castellon, et al., ACS Sustain. Chem. Eng. 10 (2022) 13835–13848.
[139] P. Salisaeng, P. Arnnok, N. Patdhanagul, R. Burakham, J. Agric. Food. Chem. 64 (2016) 2145–2152.
[140] C.S. Cao, S.M. Xia, Z.J. Song, et al., Angew. Chem. Int. Ed. 59 (2020) 8586–8593.
[141] M. Chen, Q. Wu, C. Lin, et al., ACS Appl. Mater. Interfaces 12 (2020) 40236–40247.
[142] M.A. Patel, F. Luo, M.R. Khoshi, et al., ACS Nano 10 (2016) 2305–2315.
[143] H. Kim, J.C. Jung, P. Kim, et al., Preparation of heteropolyacid/carbon catalyst and its application to methacrolein oxidation, in: E.M. Gaigneaux, M. Devillers, D.E. De Vos, et al. (Eds.), Studies in Surface Science and Catalysis, Elsevier Inc., 2006, pp. 801–808.